ISSN 2096-7071
CN 10-1629/R1

CHINA CDC WEEKLY

Vol. 3 No. 46 Nov. 12, 2021

中国疾病预防控制中心周报

COVID-19 ISSUE (20)

ISSN 2096-7071

China CDC Weekly

Cover photo: A reemergent confirmed domestic case of COVID-19 related to cold-chain food products in Dalian City, Liaoning Province, November 4, 2021.

Methods and Applications

Machine Learning Approach Effectively Predicts Binding Between SARS-CoV-2 Spike and ACE2 Across Mammalian Species — Worldwide, 2021

Yue Ma[1,&]; Yu Hu[1,2,&]; Binbin Xia[1]; Pei Du[1]; Lili Wu[1]; Mifang Liang[3]; Qian Chen[1,4]; Huan Yan[5]; George F. Gao[1]; Qihui Wang[1,#]; Jun Wang[1,#]

ABSTRACT

Introduction: Severe acute respiratory syndrome coronavirus 2 (SARS-CoV-2) is a recently emergent coronavirus of natural origin and caused the coronavirus disease (COVID-19) pandemic. The study of its natural origin and host range is of particular importance for source tracing, monitoring of this virus, and prevention of recurrent infections. One major approach is to test the binding ability of the viral receptor gene ACE2 from various hosts to SARS-CoV-2 spike protein, but it is time-consuming and labor-intensive to cover a large collection of species.

Methods: In this paper, we applied state-of-the-art machine learning approaches and created a pipeline reaching >87% accuracy in predicting binding between different ACE2 and SARS-CoV-2 spike.

Results: We further validated our prediction pipeline using 2 independent test sets involving >50 bat species and achieved >78% accuracy. A large-scale screening of 204 mammal species revealed 144 species (or 61%) were susceptible to SARS-CoV-2 infections, highlighting the importance of intensive monitoring and studies in mammalian species.

Discussion: In short, our study employed machine learning models to create an important tool for predicting potential hosts of SARS-CoV-2 and achieved the highest precision to our knowledge in experimental validation. This study also predicted that a wide range of mammals were capable of being infected by SARS-CoV-2.

INTRODUCTION

Severe acute respiratory syndrome coronavirus 2 (SARS-CoV-2) has caused the ongoing pandemic of coronavirus disease (COVID-19) and has led to more than 229 million people infected and 4.7 million fatalities as of September 23, 2021 (https://covid19.who.int). Despite a large number of investigations on the biology and pathology of SARS-CoV-2, as well as treatment of COVID-19, the virus and pandemic still pose a tremendous threat to global health and stability. The natural origin of this virus has gained consensus among scientific communities but available evidence is still short of being conclusive. For instance, bats and pangolins have been proposed but disputes still remain (*1*), leaving room for misinformation and abuse. Identifying the host species susceptible to, including the source and intermediate species of, SARS-CoV-2 is still one of the central scientific objectives for COVID-19 research and will help provide information for monitoring and containing a potential viral reservoir as well as preventing reoccurring zoonosis as in the case of influenza viruses.

The entry of SARS-CoV-2 to host cells requires the binding of its spike protein and host angiotensin I converting enzyme 2 (ACE2), a process that underwent intense investigation. Blocking their binding with a list of neutralizing monoclonal antibodies (mAbs) has been demonstrated to effectively prevent viral entry to cells *in vitro* and *in vivo* (*2*), and several mAbs were approved for clinical treatment of COVID patients (*3*). Short peptide mimicking the structure of ACE2 region binding to the viral spike protein has also been developed, which binds the receptor binding domain (RBD) of spike proteins with picomole-level affinity and effectiveness in cell assays (*4*). Besides serving as a target for treatment, the ability of binding between the SARS-CoV-2 spike and the ACE2 from non-human species indicated the susceptibility of those species towards SARS-CoV-2 and, combined with ecological data and evolutionary evidence, might identify key species as probable origins and/or intermediate hosts of SARS-CoV-2.

Screening the binding between the ACE2 from large-scale collection of species and the SARS-CoV-2 spike protein thus is highly desired; however, in reality,

there are great constraints due to costs and time required for experimental verification. Alternatively, bioinformatic approaches capable of predicting binding between the two proteins with high precision are helpful in prioritizing species of interest and excluding very unlikely species, reducing the cost and time for this purpose. Based on sequence similarity in the ACE2 across species, Damas et al. (*5*) proposed a score predicting binding to the SARS-CoV-2 spikes; since then, many species' ACE2 have been tested, and retrospectively it is clear that the approach is limited in its precision. Namely, ACE2 from all bat species (36 in total in their prediction) were predicted to be "low" or "very low" in binding to the SARS-CoV-2 spike, but later experiments demonstrated that 20 species' ACE2 (55.56%) could bind to the viral spike (*6*). Alongside bats, 17 out of 29 (58.62%) other mammals with ACE2 genes considered unlikely to bind to the SARS-CoV-2 spike actually had ability to bind as well (Supplementary Table S1, available in http://weekly.chinacdc.cn/). Thus, the currently available bioinformatic approach has an extremely high false negative rate and is still short of precisely predicting binding between the SARS-CoV-2 spike protein and the ACE2 across species.

METHODS

We have therefore applied machine learning approaches to address the remaining challenges (see Supplementary Materials, available in http://weekly.chinacdc.cn/). Machine learning methods have the ability to combine diverse and complex data and automatically learn features for prediction, classification, and regressions. In biology, they have been successfully applied in establishing predictive and classification models using genomic features (*7*), metabolic markers (*8*), and many more (*9*). In our study, we selected five representative machine learning methods to perform classification (i.e., prediction of binding *vs.* non-binding), namely Support Vector Machine (SVM), Decision Tree (DT), Random Forest (RF), Adaboost (ADA), and Gradient Boosting Regression Tree (GBRT). For the single estimator we chose SVM and DT because they are suitable for small training sets. However, single estimators have a tendency to cause poor generalizability or robustness. To reduce this issue, we chose three additional ensemble methods (RF, ADA, and GBRT) for the construction of the prediction model.

The five models were further equipped with *a priori* information to establish a combined prediction pipeline. A study on the human ACE2 introduced mutations at 117 amino acid (AA) sites individually, whereas at each site the AA was mutated to all potential alternative AAs and the changes in affinity (relative to the wildtype ACE2) to that of SARS-CoV-2 have been experimentally examined, providing a quantitative reference data (*10*). Further, studies from Wang et al. (*11*) and Liu et al. (*12*) identified subsets of 24 and 20 AAs, respectively, in the human ACE2 as important sites for interaction with SARS-CoV-2 spike protein, which can be used as qualitative information to reduce model complexity and potential over-fitting. Based on reported experimental verifications of the ACE2 protein from 90 species (73 unique species, 27 from Wu et al. (*13*), 49 from Liu et al. (*12*). 14 are from our lab and currently being considered for independent publication), we aligned the ACE2 sequences of those species to the human ACE2 and extracted AAs to replace with log2 enrichment ratios for the 117, 24, and 20 sites as input data format (Figure 1A). We have deposited this pipeline and details of the method at https://github.com/mayuefine/Binding-prediction.

RESULTS

The training and the test set data contained 62 and 11 species, respectively, and the test set was set aside from the training process. In order to screen the models with a stable performance, we trained five models on three groups of site information (group 20, group 24, and group 117, each group containing 5 machine learning approaches). Finally, the predictions of the three groups were combined and a combination of six models with the highest precision was chosen as our prediction pipeline, out of a total of 408 combinations; this pipeline reached an in silico precision of circa 87.5% (Figure 1B) and was used for subsequent analysis. We used this pipeline to generate a prediction score for each ACE2 sequence, which was equal to the number of models predicting that it binded to the viral spike divided by the total number of models.

Bat species of the order Chiroptera were of highest interest for tracing the origin and studying the host range of SARS-CoV-2, as bat species harbor multiple coronavirus species including the SARS virus. One of the closest related strains of coronavirus to SARS-CoV-2, RaTG13, was found in horseshoe bats (*Rhinolophus affinis*) (*14*). Thus, we applied our pipeline and

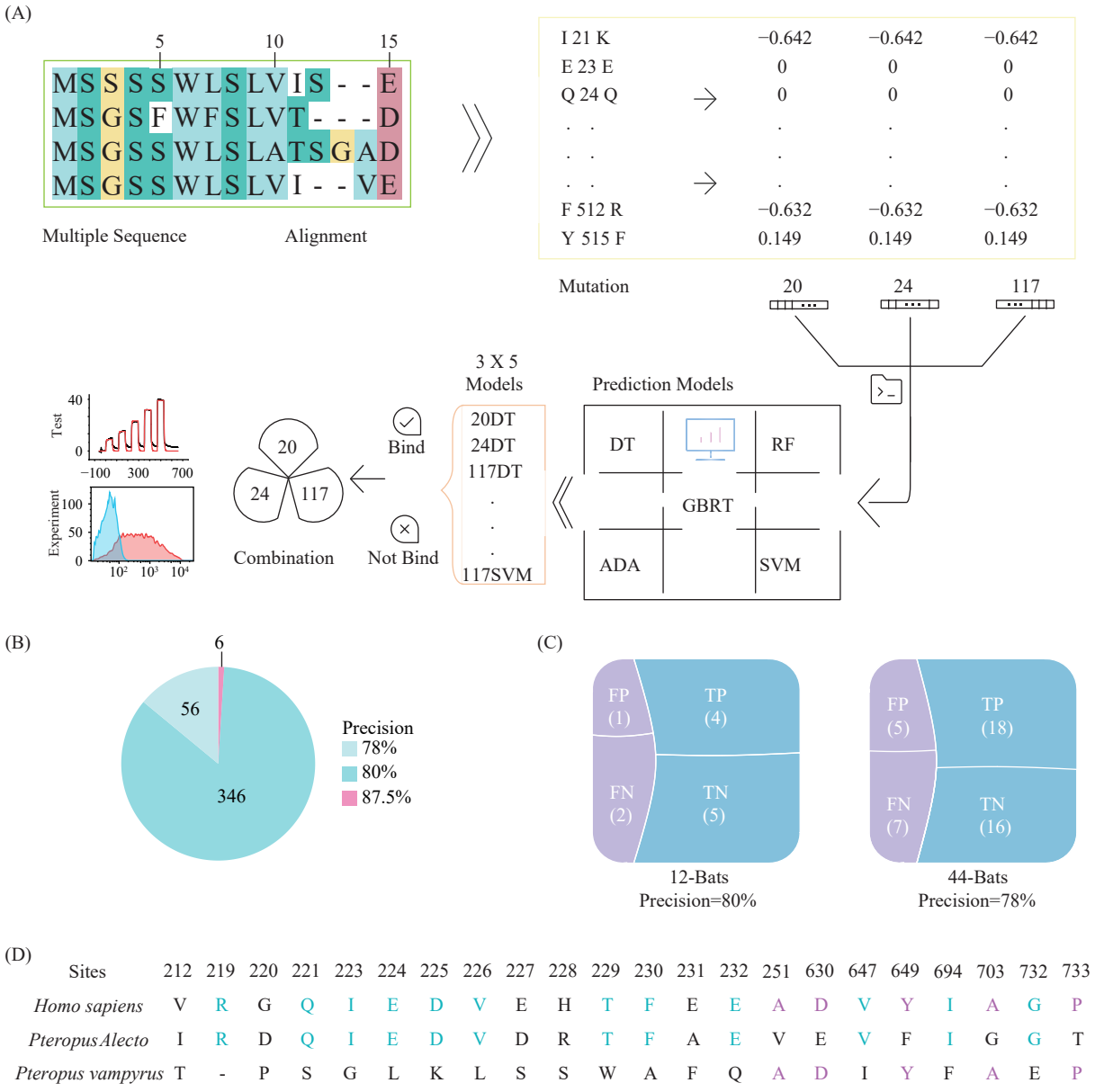

FIGURE 1. Overview of methodology and model performance of this study. (A) Schematic representation of the workflow; (B) The distribution of precision from all 408 potential combinations of models/input data; (C) Distribution of true positive (TP), true negative (TN), false positive (FP), and false negative (FN) in our models' prediction in two experimentally validated datasets; (D) Distribution of different AAs in human (*Homo sapiens*) and two bat species (*P. alecto* and *P. vampyrus*).

Note: After sequencing alignment, information from chosen sites were transformed into vectors and fed to five different models, from which the optimal combination was chosen as pipeline and used to predict available ACE2 sequences. After the prediction, we selected some of the sequences for experimental validation. Figure 1B showed that multiple combinations reached high precision using our testing dataset. that we presume to influence binding between ACE2 and viral spike protein as well, based on the observation that the two bat species' ACE2 have different binding with the viral spike.

Abbreviations: ACE2=angiotensin I converting enzyme 2; DT=decision tree; RF=random forest; GBRT=gradient boosting regression tree; ADA=adaboost; SVM=support vector machine.

examined across bat species with ACE2 sequences available (59 in total), in which we predicted their ability to bind with SARS-CoV-2 spike proteins. We then tested the precision of our prediction in two experimentally validated datasets, in which ACE2 with predictions score >0.5 were considered likely to bind to the viral spike. We selected 12 bats' ACE2 and expressed the proteins, then confirmed with Surface Plasmon Resonance (SPR) and flow cytometry for the ability to bind the viral spike (Supplementary

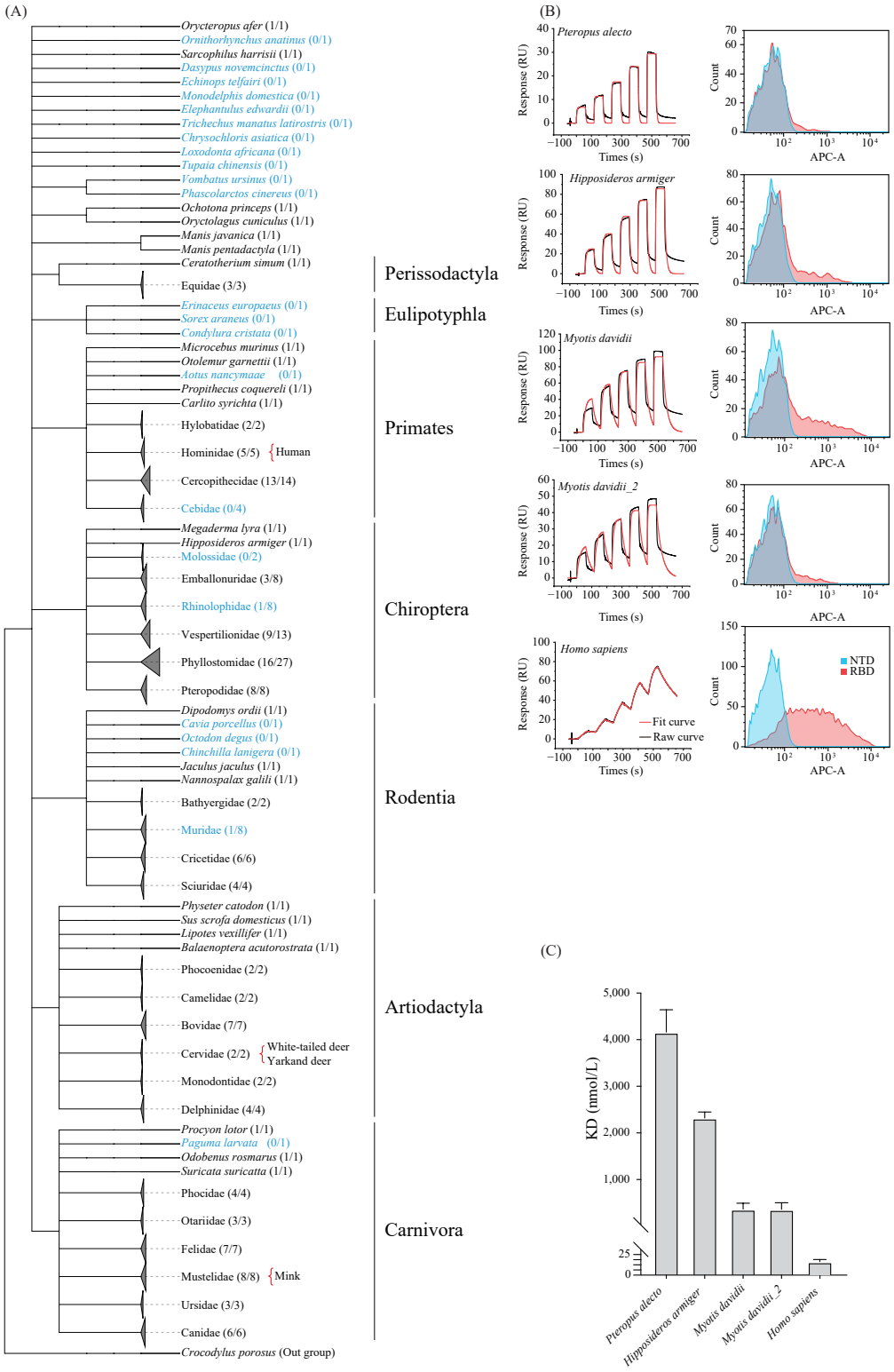

FIGURE 2. Prediction and validations of ACE2 across species in binding to SARS-CoV-2 spike. (A) The predicted range of species with ACE2 capable of binding to SARS-CoV-2; (B) SPR and flow cytometry validation for multiple species' ACE2 in binding to SARS-CoV-2 spike; (C) KD in nmol/L of the species shown in (B).
Note: For families with multiple species, the branch is collapsed and the proportion predicted to bind is shown in Figure 2A. Blue species/families are those predicted not to bind.
Abbreviations: ACE2=angiotensin I converting enzyme 2; SARS-CoV-2=severe acute respiratory syndrome coronavirus 2; SPR=surface plasmon resonance; KD=binding affinity.

Table S2, available in http://weekly.chinacdc.cn/). Overall, 4 of the 6 ACE2s predicted to bind to the SARS-CoV-2 spike were validated to bind to the viral spike (Figure 2B and Supplementary Figure S1, available in http://weekly.chinacdc.cn/), together with 5 ACE2s confirmed not to bind out of 6 ACE2s predicted to be so. Here we achieved a precision of 80% (Figure 1C). Then, using another dataset of 46 bat species by Yan et al. (*6*), after excluding the 2 sequences contained in our training set, we predicted the binding capacity and achieved 78.26% precision as shown in Figure 1C. Thus, our unified pipeline incorporating multiple machine learning models and different sets as input has the ability of confidently predicting binding between bat ACE2s and viral spikes.

It also drew our attention that during our validation, ACE2 sequences from *Pteropus alecto* and *Pteropus vampyrus* have identical AAs at all 117 sites we selected for input; however, *P. alecto* ACE2 could bind to the SARS-CoV-2 spike in our experimental system and *P. vampyrus* ACE2 had no detectable binding, suggesting additional AAs affected the binding capacity. We compared ACE2 sequences of these 2 species and identified in total 22 sites of difference between the 2. Of these sites, 16 are identical to human ACE2 (12 for *P. alecto and 4 for P. vampyrus*) (Figure 1D and Figure 2C). This comparison provided extra information that one or more of the AAs different between *P. alecto* and *P. vampyrus* and humans underly the differences in binding to the viral spike protein but have not been discovered in available studies. Closer investigations revealed that this set of AAs was not involved in binding with viral spike protein, thus their influences were indirect and likely affected by the ACE2 protein structurally or even by post-translation modifications including glycosylation.

Eventually, we refined our models incorporating the modified list of AAs as an input, and performed predictions on available ACE2 sequences from mammalian species (Supplementary Table S3, available in http://weekly.chinacdc.cn/, 204 in total and belonging to 69 families). This has resulted in the ACE2 of interest (likely to bind to the SARS-CoV-2 spike) from a total of 144 species, spread across 47 families (60.87%, Figure 2A). It is worth noting that the wide range of potential mammalian hosts agree with the emerging evidences of SARS-CoV-2 virus presence across mammals. Aside from 5 species of Hominidae (primates), ACE2s were predicted to bind to the viral spike protein in: 13 species of Cercopithecidae (old world monkeys), 8 species of Pteropodidae (old world fruit bats), 7 species of Felidae (cats), 7 species of Bovidae (ruminants), 7 species of Mustelidae (containing minks), 6 species of Canidae (dogs), 3 species of Equidae (horses), 6 species of Cricetidae (muroid rodents), 4 species of Sciuridae (squirrels), and 3 species of Ursidae (bears). Even in all 3 families of marine mammal, their ACE2s had high likelihood to bind to the SARS-CoV-2 spike (in all 4 species of Phocidae, 4 of Delphinidae and 3 of Otariidae, Figure 2B). Our prediction was supported by emerging reports that white-tailed deer (family Cervidae) were positive in antibodies against SARS-CoV-2 in 2021, which came in addition to reports of dogs, cats, and minks being viable hosts for this virus. In summary, based on ACE2 sequence features, our study suggested that SARS-CoV-2 has an extremely large range of potential hosts and indicates the importance of investigating wild animals for viral existence and monitoring its spread.

DISCUSSION

In conclusion, our study employed machine learning models suitable for analyzing sequence data, incorporated established functional data with multiple features extracted from sequences, and achieved high precision in predicting binding between ACE2s from difference species to the spike protein of SARS-CoV-2. The precision within the test data set was 87.5%, and in a total of 44 bat species, the group of mammals that attracted most concern, we achieved >78% precision as well, indicating that the model can be further expanded to predict susceptibility of more bat species once genomic sequences or ACE2 sequences become available (Supplementary Table S4, available in http://weekly.chinacdc.cn/). With the same approach we have also screened the available ACE2 sequences across a large range of mammals, in which we found that a large range of mammals requires attention. Our pipeline is capable of determining species of interest for tracing and analyzing species of interest to understand the potential origin of and transmission routes of SARS-CoV-2.

Our pipeline, in terms of performance, remains to be improved upon, provided that more accurate machine-learning models and/or more a priori information continues to emerge. First, limited by the number of experimentally validated sets and understanding on ACE2-spike interactions, we had to limit the total AAs in the ACE2 sequences for training and prediction, in which our result already indicated

contained critical information that is currently unavailable with regard to AAs in other part of the sequence, as in the case of *P. alecto* and *P. vampyrus*. In addition, the growing concerns amid the COVID-19 pandemic lie in the fast-emerging variants of SARS-CoV-2 strains, especially when mutations in ACE2-interacting AAs in the spike protein have already demonstrated changes in binding affinity to human ACE2s, whether they lead to host range changes and even broader transmission remain to be investigated.

In summary, our approach has the potential and will need to be expanded to analyze binding abilities of different SARS-CoV-2 variants and ACE2s to forecast the potential spread of this virus and identify priority species for monitoring.

Funding: The Strategic Priority Research Programs of the Chinese Academy of Sciences (XDB29020000), the National Natural Science Foundation of China (32041009) and Key R&D Program of Shandong Province (2020CXGC011305).

doi: 10.46234/ccdcw2021.235

[#] Corresponding authors: Jun Wang, junwang@im.ac.cn; Qihui Wang, wangqihui@im.ac.cn.

[1] CAS Key Laboratory of Pathogen Microbiology and Immunology, Institute of Microbiology, Chinese Academy of Sciences, Beijing, China; [2] School of Life Sciences, Division of Life Sciences and Medicine, University of Science and Technology of China, Hefei, Anhui, China; [3] State Key Laboratory for Molecular Virology and Genetic Engineering, National Institute for Viral Disease Control and Prevention, Chinese Center for Disease Control and Prevention, Beijing, China; [4] Institute of Physical Science and Information, Anhui University, Hefei, Anhui, China; [5] State Key Laboratory of Virology, Modern Virology Research Center, College of Life Sciences, Wuhan University, Wuhan, Hubei, China.
[&] Joint first authors.

Submitted: October 23, 2021; Accepted: November 01, 2021

REFERENCES

1. Wacharapluesadee S, Tan CW, Maneeorn P, Duengkae P, Zhu F, Joyjinda Y, et al. Evidence for SARS-CoV-2 related coronaviruses circulating in bats and pangolins in Southeast Asia. Nat Commun 2021;12(1):972. http://dx.doi.org/10.1038/s41467-021-21240-1.
2. Kreye J, Reincke SM, Kornau HC, Sánchez-Sendin E, Corman VM, Liu HJ, et al. A therapeutic non-self-reactive SARS-CoV-2 antibody protects from lung pathology in a COVID-19 hamster model. Cell 2020;183(4):1058 – 69.e19. http://dx.doi.org/10.1016/j.cell.2020.09.049.
3. U.S. Food & Drug Administration. Coronavirus (COVID-19) update: FDA authorizes monoclonal antibody for treatment of COVID-19. 2020. https://www.fda.gov/news-events/press-announcements/coronavirus-covid-19-update-fda-authorizes-monoclonal-antibody-treatment-covid-19. [2021-8-22].
4. Cao LX, Goreshnik I, Coventry B, Case JB, Miller L, Kozodoy L, et al. De novo design of picomolar SARS-CoV-2 miniprotein inhibitors. Science 2020;370(6515):426 – 31. http://dx.doi.org/10.1126/science.abd9909.
5. Damas J, Hughes GM, Keough KC, Painter CA, Persky NS, Corbo M, et al. Broad host range of SARS-CoV-2 predicted by comparative and structural analysis of ACE2 in vertebrates. Proc Natl Acad Sci USA 2020;117(36):22311 – 22. http://dx.doi.org/10.1073/pnas.2010146117.
6. Yan H, Jiao HW, Liu QY, Zhang Z, Xiong Q, Wang BJ, et al. ACE2 receptor usage reveals variation in susceptibility to SARS-CoV and SARS-CoV-2 infection among bat species. Nat Ecol Evol 2021;5(5):600 – 8. http://dx.doi.org/10.1038/s41559-021-01407-1.
7. Huang SJ, Cai NG, Pacheco PP, Narrandes S, Wang Y, Xu W. Applications of support vector machine (SVM) learning in cancer genomics. Cancer Genomics Proteomics 2018;15(1):41 – 51. http://dx.doi.org/10.21873/cgp.20063.
8. Liang L, Rasmussen MLH, Piening B, Shen XT, Chen SJ, Röst H, et al. Metabolic dynamics and prediction of gestational age and time to delivery in pregnant women. Cell 2020;181(7):1680 – 92.e15. http://dx.doi.org/10.1016/j.cell.2020.05.002.
9. Toth R, Schiffmann H, Hube-Magg C, Büscheck F, Höflmayer D, Weidemann S, et al. Random forest-based modelling to detect biomarkers for prostate cancer progression. Clin Epigenetics 2019;11(1):148. http://dx.doi.org/10.1186/s13148-019-0736-8.
10. Chan KK, Dorosky D, Sharma P, Abbasi SA, Dye JM, Kranz DM, et al. Engineering human ACE2 to optimize binding to the spike protein of SARS coronavirus 2. Science 2020;369(6508):1261 – 5. http://dx.doi.org/10.1126/science.abc0870.
11. Wang QH, Zhang YF, Wu LL, Niu S, Song CL, Zhang ZY, et al. Structural and functional basis of SARS-CoV-2 entry by using human ACE2. Cell 2020;181(4):894 – 904.e9. http://dx.doi.org/10.1016/j.cell.2020.03.045.
12. Liu YH, Hu GW, Wang YY, Ren WL, Zhao XM, Ji FS, et al. Functional and genetic analysis of viral receptor ACE2 orthologs reveals a broad potential host range of SARS-CoV-2. Proc Natl Acad Sci USA 2021;118(12):e2025373118. http://dx.doi.org/10.1073/pnas.2025373118.
13. Wu LL, Chen Q, Liu KF, Wang J, Han PC, Zhang YF, et al. Broad host range of SARS-CoV-2 and the molecular basis for SARS-CoV-2 binding to cat ACE2. Cell Discov 2020;6:68. http://dx.doi.org/10.1038/s41421-020-00210-9.
14. Liu KF, Pan XQ, Li LJ, Yu F, Zheng AQ, Du P, et al. Binding and molecular basis of the bat coronavirus RaTG13 virus to ACE2 in humans and other species. Cell 2021;184(13):3438 – 51.e10. http://dx.doi.org/10.1016/j.cell.2021.05.031.

Supplementary Material

Method

Data Collection

The 73 species angiotensin I converting enzyme 2 (ACE2) sequences for constructing predictive models and evaluation were collected from published articles (*1*–*2*) and unpublished data. Overall, 11 sequences from these 73 were randomly selected as test dataset for model evaluation and were not involved in model training.

The sequences of mammalian ACE2 for prediction were downloaded as of September 22, 2020 with a total of 294 ACE2 sequences of mammalian species from 23 orders being gathered. We performed multiple sequence alignment on collection of 294 sequences with human ACE2 sequence, using software CLUSTAL (version 2.1, Conway Institute, UCD, Dublin, Ireland, parameter "complete multiple alignment") (*3*), in which sequences with more than 10 consecutive amino acid missing in the head 100 sites were excluded from the subsequent analysis, resulting in 272 ACE2 sequences (204 unique species).

Model Construction and Evaluation

We selected key amino acid sites and used the log2 enrichment ratios values from Chan et al. to label the amino acids for each ACE2 sequence (*4*), with 20, 24, and 117 sites selected from Liu et al. (*1*), Wang et al. (*2*), and Chan et al. (*4*), respectively. The sequences screened for these three sites were divided into a training dataset and a test dataset with an 8∶2 ratio and used for training and testing of the model, respectively. As for prediction models, we used five different methods to train three different collections of sites, including support vector machine (SVM), Decision Tree, Random Forest, AdaBoost and Gradient Boosting, resulting in 15 models of input data/methods. After hundreds of epochs of training, random combinations of the 15 models were evaluated based on precision (Precision=TP/(TP+FP), where TP: True Positive, FP: False Positive). We selected six model combinations for ACE2 sequences prediction in the subsequent analysis and set the prediction score (Prediction Score=Pn/Mn), where Pn indicated the number of one sequence that was predicted to have binding ability and Mn was the total number of models used for prediction. The threshold value for the prediction score was set to 0.5, i.e., a prediction score ≥0.5 was considered to have the ability to bind with Severe acute respiratory syndrome coronavirus 2 (SARS-CoV-2). The 272 sequences were also screened for sites for binding ability prediction.

Model construction and prediction were carried out based on the scikit-learn module in the Python3 (version 0.22.2, Python Software Foundation, Fredericksburg, VA, USA). The functions used for model training were "svm," "DecisionTreeClassifier," "RandomForestClassifier," "AdaBoostClassifier," and "GradientBoostingClassifier." The parameters used for SVM were: gamma='scale'; class_weight={0:2}; for decision tree classifier were default parameters; for random forest classifier were the following: n_estimators=600, oob_score=True, n_jobs=-1, class_weight={0:2}; for Ada boost classifier were the following: base_estimator=DecisionTreeClassifier (max_depth=2), n_estimators=500; and for gradient boosting classifier were the following: n_estimators=100, learning_rate=1.0, max_depth=1, random_state=0. All details were also available in our github depository.

ACE2 Sequence Acquisition and Gene cloning

Twelve bat orthologs were randomly selected from the test sets. The full-length coding sequences (accession numbers are shown in Supplementary Table S2) of these orthologs were synthesized and cloned into the pEGFP-N1 vector for flow cytometry (FACS). The extracellular domain of these ACE2 orthologs was fused with the Fc domain of mouse IgG (mFc) and cloned into the pCAGGS expression vector for surface plasmon resonance (SPR).

Protein Expression and Purification

The SARS-CoV-2 receptor-binding domain (RBD) and SARS-CoV-2 N-terminal domain (NTD) proteins used for flow cytometry and SPR were expressed and purified from the supernatants of HEK293F cells culture as described in our previous work (*5*). Proteins were stored in a PBS buffer [1.8 mmol/L KH_2PO_4, 10 mmol/L Na_2HPO_4 (pH 7.4), 137 mmol/L NaCl, 2.7 mmol/L KCl] buffer. The indicated pCAGGS plasmids were transiently transfected into HEK293T cells (ATCC CRL-3216). Supernatants containing mFc-tagged ACE2 proteins were collected and concentrated at 48 h post-transfection.

SUPPLEMENTARY TABLE S1. Binding ability of various mammalian ACE2, including published experimental results, prediction from Damas et al. (*7*) using our method.

Mammals	Species	Common name	Experiment results	Previous prediction results	Our prediction	Accession Number
Bats	*Anoura caudifer*	Tailed tailless bat	Binding	Very low	Binding	GCA_004027475.1
	Artibeus jamaicensis	Jamaican fruit-eating bat	Binding	Very low	Binding	GCA_004027435.1
	Carollia perspicillata	Seba's short-tailed bat	Binding	Very low	Not bind	GCA_004027735.1
	Desmodus rotundus	Common vampire bat	Binding	Very low	Not bind	XP_024425698.1
	Eidolon helvum	Straw-colored fruit bat	Binding	Low	Binding	GCA_000465285.1
	Eonycteris spelaea	Lesser dawn bat	Binding	Low	Binding	GCA_003508835.1
	Macroglossus sobrinus	Long-tongued fruit bat	Binding	Very low	Binding	GCA_004027375.1
	Megaderma lyra	Indian false vampire	Binding	Low	Binding	MT515624
	Micronycteris hirsuta	Hairy big-eared bat	Binding	Very low	Not bind	GCA_004026765.1
	Miniopterus schreibersii	Schreibers' long-fingered bat	Binding	Very low	Binding	GCA_004026525.1
	Mormoops blainvillei	Antillean ghost-faced bat	Binding	Very low	Not bind	GCA_004026545.1
	Myotis brandtii	Brandt's bat	Binding	Very low	Binding	XP_014399780.1
	Myotis davidii	David's myotis	Binding	Very low	Binding	XP_006775273.1
	Myotis lucifugus	Little brown bat	Binding	Very low	Binding	XP_023609437.1
	Myotis myotis	Greater mouse-eared bat	Binding	Very low	Binding	https://vgp.github.io/genomeark/Myotis_myotis
	Noctilio leporinus	Greater bulldog bat	Binding	Very low	Binding	GCA_004026585.1
	Pipistrellus pipistrellus	Common pipistrelle	Binding	Very low	Not bind	GCA_004026625.1
	Pteropus alecto	Black flying fox	Binding	Low	Binding	XP_006911709.1
	Rousettus aegyptiacus	Egyptian rousette	Binding	Low	Binding	XP_015974412.1
	Tadarida brasiliensis	Brazilian free-tailed bat	Binding	Very low	Not bind	GCA_004025005.1
Other Mammals	*Ailuropoda melanoleuca*	Giant panda	Binding	Low	Binding	XP_002930657.1
	Camelus ferus	Wild Bactrian camel	Binding	Low	Binding	XP_006194263.1
	Ceratotherium simum simum	Southern white rhinoceros	Binding	Low	Binding	XP_004435206.1
	Equus caballus	Horse	Binding	Low	Binding	XP_001490241.1
	Peromyscus leucopus	White-footed mouse	Binding	Low	Binding	XP_028743609.1
	Rousettus aegyptiacus	Egyptian rousette	Binding	Low	Binding	XP_015974412.1
	Sus scrofa	Pig	Binding	Low	Binding	NP_001116542.1
	Ursus arctos horribilis	Grizzly bear	Binding	Low	Binding	XP_026333865.1
	Vulpes vulpes	Red fox	Binding	Low	Binding	XP_025842512.1
	Callorhinus ursinus	Northern fur seal	Binding	Very low	Binding	XP_025713397.1
	Eumetopias jubatus	Steller sea lion	Binding	Very low	Binding	XP_027970822.1
	Jaculus jaculus	lesser Egyptian jerboa	Binding	Very low	Binding	XP_004671523.1
	Manis javanica	Malayan pangolin	Binding	Very low	Binding	XP_017505746.1
	Mustela erminea	Stoat	Binding	Very low	Binding	XP_032187677.1
	Myotis lucifugus	Little brown bat	Binding	Very low	Binding	XP_023609437.1
	Neomonachus schauinslandi	Hawaiian monk seal	Binding	Very low	Binding	XP_021536480.1
	Zalophus californianus	California sea lion	Binding	Very low	Binding	XP_027465353.1

Abbreviations: ACE2=angiotensin I converting enzyme 2.

SUPPLEMENTARY TABLE S2. Results of binding between ACE2 from 12 bat species and SARS-CoV-2 spike performed in our study.

Species	KD (nmol/L)	Prediction score	Accession number
Pteropus alecto	4,163.47±479.62	1.00	XP_006911709.1
Pteropus vampyrus	–*	1.00	XP_011361275.1
Hipposideros armiger	2,323.89±124.60	0.70	XP_019522936.1
Myotis davidii	369.03±126.37	0.79	XP_015426919.1
Myotis davidii	361.33±144.51	0.79	XP_006775273.1
Rhinolophus pearsonii	–	0.20	ABU54053.1
Megaderma lyra	735.58±121.91	0.47	QKE49998.1
Molossus molossus	–	0.33	KAF6491643.1
Pipistrellus abramus	–	0.11	ACT66266.1
Rhinolophus landeri	3,635.83±156.31	0.01	ALJ94034.1
Scotophilus dinganii	–	0.22	QJF77809.1
Tadarida brasiliensis	–	0.17	QLF98520.1
Homo sapiens	13.28±2.06	1.00	NP_00135844.1

Note: Prediction score of >0.5 is considered to be able to bind SARS-CoV-2 spike.
Abbreviations: ACE2=angiotensin I converting enzyme 2; SARS-CoV-2=severe acute respiratory syndrome coronavirus 2; KD=binding affinity.
* No detected affinity.

Flow Cytometry Analysis

To test the binding between each of the 12 ACE2s and SARS-CoV-2 RBD, the 12 bat ACE2s fused with eGFP were expressed on the cell surface by transfecting each of the 12 pEGFP-N1-ACE2s plasmids into BHK21 cells (ATCC, ATCC CCL-10) using PEI (Alfa). Cell culture was replaced with fresh media (DMEM with 10% FBS, Gibco) 4–6 h post-transfection. After 48 h, cells were collected and resuspended in PBS. Then, 2×10^5 cells were incubated with the histidine tagged test proteins (SARS-CoV-2 RBD, SARS-CoV-2 NTD) at a concentration of 10 μg/mL at 37 °C for 30 min. Cells were then washed three times in PBS and stained with anti-His/APC antibodies (1:500, Miltenyi Biotec, AB_2751870) for 30 min at 37 °C. Flow cytometry (FACS) data were acquired on a BD FACSCanto (BD Biosciences, Franklin Lakes, NJ, USA) and analyzed using FlowJo V10 software (TreeStar Inc., Ashland, OR, USA), with results shown in Supplementary Figure S1.

SPR Analysis

We tested the binding affinities between the mFc-tagged ACE2s and SARS-CoV-2 RBD or SARS-CoV RBD proteins by SPR using a BIAcore 8K (GE Healthcare) carried out at 25 °C in single-cycle mode. The PBST buffer (1.8 mmol/L KH_2PO_4, 10 mmol/L Na_2HPO_4 (pH 7.4), 137 mmol/L NaCl, 2.7 mmol/L KCl, and 0.05% (v/v) Tween 20) was used as the running buffer. The CM5 biosensor chip was first immobilized with anti-mIgG antibody (ZSGB-BIO, ZF-0513) as previously described. (*1*) The supernatants containing mFc-tagged ACE2s were injected and captured by the antibody immobilized on the CM5 chip at approximately 300-600 response units. The serially diluted SARS-CoV-2 RBD protein flowed over the chip surface, with another channel set as control. The chip was regenerated using pH 1.7 glycine after each reaction. The equilibrium dissociation constants (binding affinity, KD) for each pair of interaction were calculated with BIAcore_8K evaluation software (GE Healthcare, Chicago, IL, USA) by fitting to a 1∶1 Langmuir binding model. Data were analyzed using OriginLab (Origin 2018, OriginLab Corporation, Northampton, MA, USA).

Phylogenetic Tree

The phylogenetic tree was constructed by uploading the species names from 272 sequences into NCBI Taxonomy Common Tree (https://www.ncbi.nlm.nih.gov/Taxonomy/CommonTree/). The visualization of the phylogenetic tree was based on iTol (*6*).

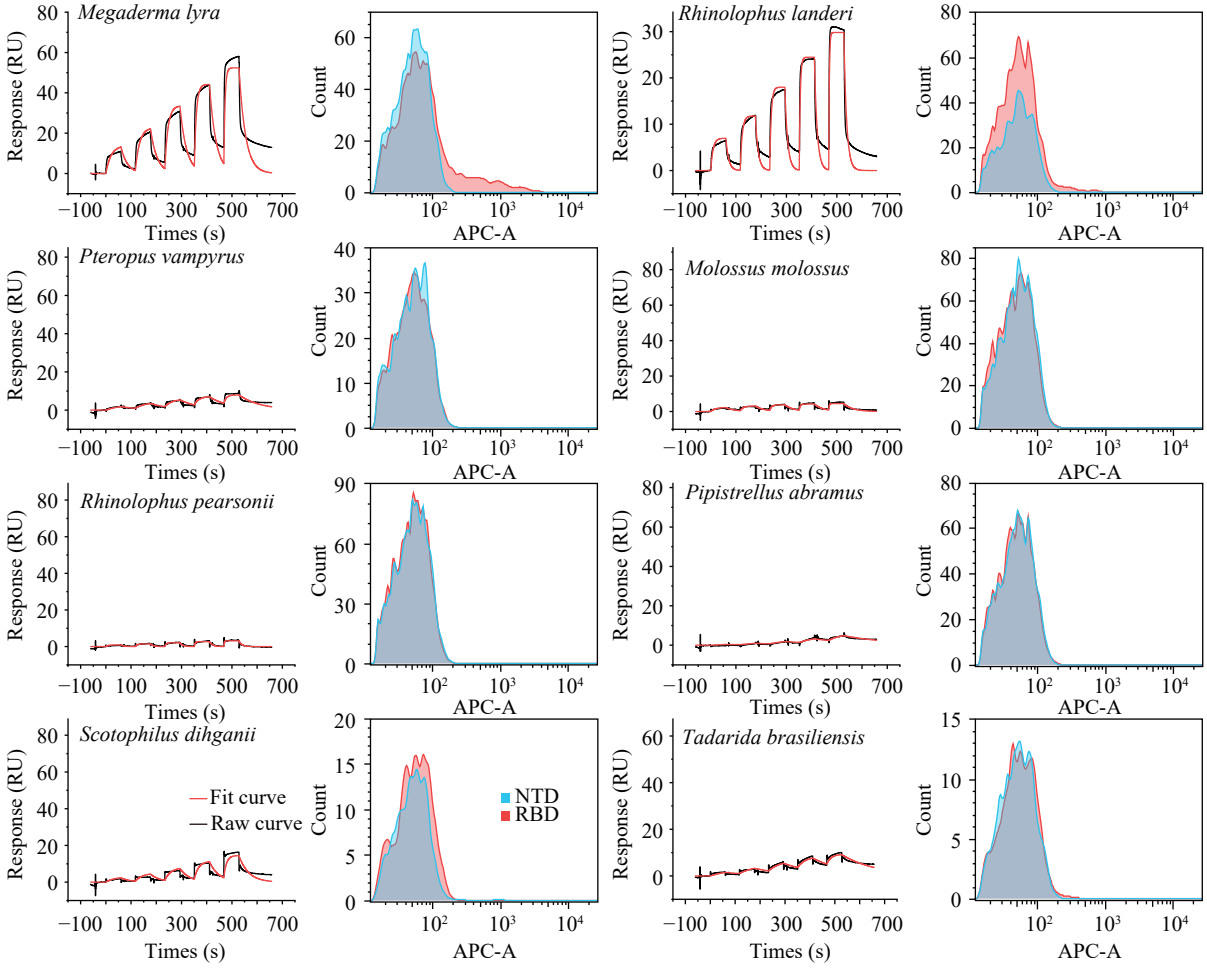

SUPPLEMENTARY FIGURE S1. SPR and flow cytometry validation for multiple species' ACE2.
Abbreviations: ACE2=angiotensin I converting enzyme 2; SPR=surface plasmon resonance; RU=response unit; NTD=N-terminal domain; RBD=receptor-binding domain.

SUPPLEMENTARY TABLE S3. Prediction of the binding capacity of collected mammalian ACE2 to SARS-CoV-2.

Species	Common name	Prediction scores	Data availability
Hylobates moloch	Silvery gibbon	1.00	XP_032612508.1
Phocoena sinus	Vaquita	1.00	XP_032476001.1
Globicephala melas	Long-finned pilot whale	1.00	XP_030703991.1
Lynx canadensis	Canada lynx	1.00	XP_030160839.1
Monodon monoceros	Narwhal	1.00	XP_029095804.1
Peromyscus leucopus	White-footed mouse	1.00	XP_028743609.1
Balaenoptera acutorostrata scammoni	Common minke whale	1.00	XP_028020351.1
Eumetopias jubatus	Steller sea lion	1.00	XP_027970822.1
Marmota flaviventris	Yellow-bellied marmot	1.00	XP_027802308.1
Zalophus californianus	California sea lion	1.00	XP_027465353.1
Bos indicus x Bos taurus	Hybrid cattle	1.00	XP_027389729.1
Bos indicus x Bos taurus	Hybrid cattle	1.00	XP_027389727.1
Cricetulus griseus	Chinese hamster	1.00	XP_027288607.1
Lagenorhynchus obliquidens	Pacific white-sided dolphin	1.00	XP_026951598.1
Acinonyx jubatus	Cheetah	1.00	XP_026910297.1
Ursus arctos horribilis	Grizzly bear	1.00	XP_026333865.1
Vulpes vulpes	Red fox	1.00	XP_025842512.1
Puma concolor	Puma	1.00	XP_025790417.1
Callorhinus ursinus	Northern fur seal	1.00	XP_025713397.1
Canis lupus dingo	Dingo	1.00	XP_025292925.1
Theropithecus gelada	Gelada	1.00	XP_025227847.1
Neophocaena asiaeorientalis asiaeorientalis	Yangtze finless	1.00	XP_024599894.1
Pongo abelii	Sumatran orangutan	1.00	XP_024096013.1
Physeter catodon	Sperm whale	1.00	XP_023971279.1
Felis catus	Domestic cat	1.00	XP_023104564.1
Piliocolobus tephrosceles	Ugandan red colobus	1.00	XP_023054821.1
Delphinapterus leucas	Beluga whale	1.00	XP_022418360.1
Papio anubis	Olive baboon	1.00	XP_021788732.1
Neomonachus schauinslandi	Hawaiian monk seal	1.00	XP_021536486.1
Neomonachus schauinslandi	Hawaiian monk seal	1.00	XP_021536480.1
Sus scrofa	Pig	1.00	XP_020935034.1
Sus scrofa	Pig	1.00	XP_020935033.1
Odocoileus virginianus texanus	White-tailed deer	1.00	XP_020768965.1
Bos indicus	Bos taurus indicus	1.00	XP_019811720.1
Bos indicus	Bos taurus indicus	1.00	XP_019811719.1
Tursiops truncatus	Common bottlenose dolphin	1.00	XP_019781177.1
Panthera pardus	Leopard	1.00	XP_019273508.1
Gorilla gorilla gorilla	Western lowland gorilla	1.00	XP_018874749.1
Manis javanica	Malayan pangolin	1.00	XP_017505746.1
Pan troglodytes	Chimpanzee	1.00	XP_016798469.1
Pan troglodytes	Chimpanzee	1.00	XP_016798468.1
Rousettus aegyptiacus	Egyptian rousette	1.00	XP_015974412.1

Continued

Species	Common name	Prediction scores	Data availability
Marmota marmota marmota	Alpine marmot	1.00	XP_015343540.1
Propithecus coquereli	Coquerel's sifaka	1.00	XP_012494185.1
Ovis aries	Sheep	1.00	XP_011961657.1
Cercocebus atys	Sooty mangabey	1.00	XP_011891198.1
Mandrillus leucophaeus	Drill	1.00	XP_011850923.1
Colobus angolensis palliatus	Angola colobus	1.00	XP_011795654.1
Macaca nemestrina	Pig-tailed macaque	1.00	XP_011733505.1
Homo sapiens	Human	1.00	XP_011543854.1
Homo sapiens	Human	1.00	XP_011543853.1
Homo sapiens	Human	1.00	XP_011543851.1
Pteropus vampyrus	Large flying fox	1.00	XP_011361275.1
Rhinopithecus roxellana	Golden snub-nosed monkey	1.00	XP_010364367.2
Pan paniscus	Pygmy chimpanzee	1.00	XP_008972437.1
Pan paniscus	Pygmy chimpanzee	1.00	XP_008972428.1
Nannospalax galili	Upper galilee mountains blind mole rat	1.00	XP_008839098.1
Ursus maritimus	Polar bear	1.00	XP_008694637.1
Chlorocebus sabaeus	Green monkey	1.00	XP_007989304.1
Lipotes vexillifer	Yangtze River dolphin	1.00	XP_007466389.1
Panthera tigris altaica	Amur tiger	1.00	XP_007090142.1
Peromyscus maniculatus bairdii	Prairie deer mouse	1.00	XP_006973269.1
Pteropus alecto	Black flying fox	1.00	XP_006911709.1
Bubalus bubalis	Water buffalo	1.00	XP_006041602.1
Bos mutus	Wild yak	1.00	XP_005903173.1
Capra hircus	Goat	1.00	XP_005701129.2
Canis lupus familiaris	Dog	1.00	XP_005641049.1
Macaca fascicularis	Crab-eating macaque	1.00	XP_005593094.1
Ictidomys tridecemlineatus	Thirteen-lined ground squirrel	1.00	XP_005316051.3
Bos taurus	Cattle	1.00	XP_005228486.1
Bos taurus	Cattle	1.00	XP_005228485.1
Mesocricetus auratus	Golden hamster	1.00	XP_005074266.1
Heterocephalus glaber	Naked mole-rat	1.00	XP_004866157.1
Ochotona princeps	American pika	1.00	XP_004597549.2
Ceratotherium simum simum	Southern white rhinoceros	1.00	XP_004435206.1
Odobenus rosmarus divergens	Pacific walrus	1.00	XP_004415448.1
Orcinus orca	Killer whale	1.00	XP_004269705.1
Cricetulus griseus	Chinese hamster	1.00	XP_003503283.1
Nomascus leucogenys	Northern white-cheeked gibbon	1.00	XP_003261132.2
Ailuropoda melanoleuca	Giant panda	1.00	XP_002930657.1
Oryctolagus cuniculus	Rabbit	1.00	XP_002719891.1
Chrysocyon brachyurus	Maned wolf	1.00	QNC68917.1
Neofelis diardi	Sunda clouded leopard	1.00	QNC68916.1
Speothos venaticus	Bush dog	1.00	QNC68915.1
Manis pentadactyla	Chinese pangolin	1.00	QLH93383.1

Continued

Species	Common name	Prediction scores	Data availability
Dobsonia viridis	Greenish naked-backed fruit bat	1.00	QJF77815.1
Syconycteris australis	Southern blossom bat	1.00	QJF77811.1
Epomophorus wahlbergi	Wahlberg's epauletted fruit bat	1.00	QJF77792.1
Homo sapiens	Human	1.00	NP_068576.1
Homo sapiens	Human	1.00	NP_001358344.1
Capra hircus	Goat	1.00	NP_001277036.1
Canis lupus familiaris	Dog	1.00	NP_001158732.1
Macaca mulatta	Rhesus monkey	1.00	NP_001129168.1
Pongo abelii	Sumatran orangutan	1.00	NP_001124604.1
Sus scrofa	Pig	1.00	NP_001116542.1
Felis catus	Domestic cat	1.00	NP_001034545.1
Bos taurus	Cattle	1.00	NP_001019673.2
Rousettus leschenaultii	Leschenault's rousette	1.00	BAF50705.1
Rousettus leschenaultii	Leschenault's rousette	1.00	ADJ19219.1
Mesocricetus auratus	Golden hamster	1.00	ACT66278.1
Felis catus	Domestic cat	1.00	ACT66276.1
Oryctolagus cuniculus	Rabbit	1.00	ACT66271.1
Sus scrofa domesticus	Domestic pig	1.00	ACT66265.1
Rhinolophus ferrumequinum	Greater horseshoe bat	1.00	ACM45790.1
Macaca mulatta	Rhesus monkey	1.00	ACI04576.1
Macaca mulatta	Rhesus monkey	1.00	ACI04571.1
Macaca mulatta	Rhesus monkey	1.00	ACI04570.1
Macaca mulatta	Rhesus monkey	1.00	ACI04569.1
Macaca mulatta	Rhesus monkey	1.00	ACI04568.1
Macaca mulatta	Rhesus monkey	1.00	ACI04567.1
Macaca mulatta	Rhesus monkey	1.00	ACI04566.1
Macaca mulatta	Rhesus monkey	1.00	ACI04564.1
Macaca mulatta	Rhesus monkey	1.00	ACI04563.1
Macaca mulatta	Rhesus monkey	1.00	ACI04562.1
Macaca mulatta	Rhesus monkey	1.00	ACI04560.1
Macaca mulatta	Rhesus monkey	1.00	ACI04559.1
Macaca mulatta	Rhesus monkey	1.00	ACI04557.1
Macaca mulatta	Rhesus monkey	1.00	ACI04556.1
Macaca mulatta	Rhesus monkey	1.00	ACI04555.1
Macaca mulatta	Rhesus monkey	1.00	ACI04554.1
Macaca mulatta	Rhesus monkey	1.00	ACI04553.1
Macaca mulatta	Rhesus monkey	1.00	ACI04552.1
Nyctereutes procyonoides	Raccoon dog	1.00	ABW16956.1
Chlorocebus aethiops	Grivet	1.00	AAY57872.1
Camelus ferus	Wild bactrian camel	0.99	XP_006194263.1
Jaculus jaculus	Lesser Egyptian jerboa	0.99	XP_004671523.1
Mirounga leonina	Southern elephant seal	0.97	XP_034852450.1
Trachypithecus francoisi	Francois's langur	0.97	XP_033056809.1

Continued

Species	Common name	Prediction scores	Data availability
Macaca mulatta	Rhesus monkey	0.97	ACI04573.1
Equus asinus	African wild ass	0.93	XP_014713133.1
Equus przewalskii	Przewalski's horse	0.93	XP_008542995.1
Orycteropus afer afer	Aardvark	0.93	XP_007951028.1
Microtus ochrogaster	Prairie vole	0.93	XP_005358818.1
Equus caballus	Horse	0.93	XP_001490241.1
Neovison vison	American mink	0.93	QPL12211.1
Arctonyx collaris	Hog badger	0.93	QLF98526.1
Cynopterus sphinx	Indian short-nosed fruit bat	0.93	QKE49997.1
Uroderma bilobatum	Tent-building bat	0.93	QJF77842.1
Platyrrhinus vittatus	Greater broad-nosed bat	0.93	QJF77835.1
Platyrrhinus helleri	Heller's broad-nosed bat	0.93	QJF77834.1
Cynopterus sphinx	Indian short-nosed fruit bat	0.93	QJF77831.1
Chiroderma villosum	Hairy big-eyed bat	0.93	QJF77830.1
Chiroderma salvini	Salvin's big-eyed bat	0.93	QJF77829.1
Artibeus phaeotis	Dwarf fruit-eating bat	0.93	QJF77823.1
Artibeus lituratus	Great fruit-eating bat	0.93	QJF77822.1
Artibeus jamaicensis	Jamaican fruit-eating bat	0.93	QJF77821.1
Phodopus campbelli	Campbell's desert hamster	0.93	ACT66274.1
Fukomys damarensis	Damara mole-rat	0.91	XP_010643477.1
Cervus hanglu yarkandensis	Yarkand deer	0.88	KAF4027296.1
Urocitellus parryii	Arctic ground squirrel	0.87	XP_026252506.1
Urocitellus parryii	Arctic ground squirrel	0.87	XP_026252505.1
Myotis lucifugus	Little brown bat	0.87	XP_023609439.1
Myotis lucifugus	Little brown bat	0.87	XP_023609437.1
Myotis brandtii	Brandt's bat	0.87	XP_014399783.1
Myotis brandtii	Brandt's bat	0.87	XP_014399782.1
Myotis brandtii	Brandt's bat	0.87	XP_014399780.1
Taphozous melanopogon	Black-bearded Tomb Bat	0.87	QJF77841.1
Taphozous theobaldi	Theobald's tomb bat	0.87	QJF77840.1
Artibeus glaucus watsoni	–*	0.87	QJF77824.1
Artibeus hartii	Little fruit-eating bat	0.86	QJF77832.1
Scotophilus kuhlii	Lesser asiatic yellow house bat	0.82	QJF77810.1
Scotophilus dinganii	Yellow-bellied house bat	0.82	QJF77809.1
Procyon lotor	Raccoon	0.80	BAE72462.1
Myotis davidii	David's myotis	0.79	XP_015426919.1
Myotis davidii	David's myotis	0.79	XP_006775273.1
Tylonycteris robustula	Greater bamboo bat	0.79	QJF77813.1
Sarcophilus harrisii	Tasmanian devil	0.77	XP_031814825.1
Dipodomys ordii	Ord's kangaroo rat	0.77	XP_012887573.1
Dipodomys ordii	Ord's kangaroo rat	0.77	XP_012887572.1
Vicugna pacos	Alpaca	0.77	XP_006212709.1
Phoca vitulina	Harbor seal	0.73	XP_032245506.1

Continued

Species	Common name	Prediction scores	Data availability
Eptesicus fuscus	Big brown bat	0.73	XP_027986092.1
Eptesicus fuscus	Big brown bat	0.73	XP_008153150.1
Megaderma lyra	Indian false vampire	0.73	QKE49998.1
Hipposideros armiger	Great roundleaf bat	0.70	XP_019522936.1
Glossophaga commissarisi	Commissaris's long-tongued bat	0.70	QJF77793.1
Microcebus murinus	Gray mouse lemur	0.69	XP_020140826.1
Carlito syrichta	Philippine tarsier	0.69	XP_008062810.1
Anoura geoffroyi	Geoffroy's tailless bat	0.67	QJF77820.1
Suricata suricatta	Meerkat	0.66	XP_029786256.1
Anoura cultrata	Handley's tailless bat	0.66	QJF77819.1
Kerivoula pellucida	Clear-winged woolly bat	0.63	QJF77795.1
Grammomys surdaster	Grammomys	0.60	XP_028617961.1
Coleura afra	African sheath-tailed bat	0.59	QJF77826.1
Neoromicia nanus	Banana bat	0.58	QJF77804.1
Otolemur garnettii	Small-eared galago	0.56	XP_003791912.1
Hylonycteris underwoodi	Underwood's long-tongued bat	0.54	QJF77833.1
Lontra canadensis	Northern American river otter	0.53	XP_032736028.1
Enhydra lutris kenyoni	Sea otter	0.53	XP_022374079.1
Enhydra lutris kenyoni	Sea otter	0.53	XP_022374078.1
Mustela lutreola	European mink	0.53	QNC68911.1
Melogale moschata	Chinese ferret-badger	0.53	QLF98521.1
Mustela putorius furo	Domestic ferret	0.53	NP_001297119.1
Mustela erminea	Stoat	0.53	XP_032187677.1
Halichoerus grypus	Gray seal	0.52	XP_035963182.1
Sturnira parvidens	−	0.51	QJF77839.1
Sturnira ludovici	Highland Yellow-shouldered Bat	0.51	QJF77838.1
Sturnira hondurensis	−	0.51	QJF77837.1
Arvicanthis niloticus	African grass rat	0.49	XP_034341939.1
Mastomys coucha	Southern multimammate mouse	0.47	XP_031226742.1
Mus pahari	Shrew mouse	0.47	XP_021043935.1
Antrozous pallidus	Pallid bat	0.47	QJF77789.1
Carollia perspicillata	Seba's short-tailed bat	0.44	QJF77828.1
Carollia castanea	Chestnut short-tailed bat	0.44	QJF77827.1
Chinchilla lanigera	Long-tailed chinchilla	0.42	XP_013362428.1
Chinchilla lanigera	Long-tailed chinchilla	0.42	NP_001269290.1
Rhinolophus sinicus	Chinese rufous horseshoe bat	0.41	ACT66275.1
Mus caroli	Ryukyu mouse	0.40	XP_021009138.1
Vampyrum spectrum	Spectral bat	0.38	QJF77843.1
Carollia sowelli	Sowell's short-tailed bat	0.38	QJF77814.1
Loxodonta africana	African savanna elephant	0.37	XP_023410960.1
Tadarida brasiliensis	Brazilian free-tailed bat	0.37	QLF98520.1
Sorex araneus	European shrew	0.36	XP_004612266.1
Elephantulus edwardii	Cape elephant shrew	0.34	XP_006892457.1

Continued

Species	Common name	Prediction scores	Data availability
Rattus norvegicus	Norway rat	0.34	NP_001012006.1
Molossus molossus	Pallas's mastiff bat	0.33	KAF6491643.1
Aeorestes cinereus	Hoary bat	0.33	QJF77796.1
Cavia porcellus	Domestic guinea pig	0.32	ACT66270.1
Rhinolophus sinicus	Chinese rufous horseshoe bat	0.31	ADN93475.1
Micronycteris schmidtorum	Schmidts's big-eared bat	0.26	QJF77799.1
Lonchophylla robusta	Orange nectar bat	0.24	QJF77797.1
Glossophaga soricina	Pallas's long-tongued bat	0.24	QJF77794.1
Miniopterus natalensis	Natal long-fingered bat	0.22	XP_016058453.1
Tupaia chinensis	Chinese tree shrew	0.22	XP_006164754.1
Dasypus novemcinctus	Nine-banded armadillo	0.22	XP_004449124.1
Rhinolophus macrotis	Big-eared horseshoe bat	0.22	ADN93471.1
Sapajus apella	Tufted capuchin	0.20	XP_032141854.1
Cebus capucinus imitator	White headed capuchin	0.20	XP_017367865.1
Condylura cristata	Star-nosed mole	0.20	XP_012585871.1
Aotus nancymaae	Ma's night monkey	0.20	XP_012290105.1
Saimiri boliviensis boliviensis	Bolivian squirrel monkey	0.20	XP_010334925.1
Callithrix jacchus	White-tufted-ear marmoset	0.20	XP_008987241.1
Emballonura alecto	Small Asian sheath-tailed bat	0.20	QJF77816.1
Mus musculus	House mouse	0.20	NP_001123985.1
Mus musculus	House mouse	0.20	ACT66269.1
Rhinolophus pearsonii	Pearson's horseshoe bat	0.20	ABU54053.1
Vombatus ursinus	Common wombat	0.19	XP_027691156.1
Phascolarctos cinereus	Koala	0.19	XP_020863153.1
Grammomys surdaster	Grammomys	0.18	XP_028636273.1
Mirounga leonina	Southern elephant seal	0.17	XP_034882212.1
Phoca vitulina	Harbor seal	0.17	XP_032285427.1
Octodon degus	Degu	0.17	XP_023569950.1
Monodelphis domestica	Gray short-tailed opossum	0.17	XP_007500942.1
Monodelphis domestica	Gray short-tailed opossum	0.17	XP_007500941.1
Monodelphis domestica	Gray short-tailed opossum	0.17	XP_007500935.1
Paguma larvata	Masked palm civet	0.17	Q56NL1.1
Phyllostomus discolor	Pale spear-nosed bat	0.16	XP_028378317.1
Desmodus rotundus	Common vampire bat	0.16	XP_024425698.1
Rhynchonycteris naso	Proboscis bat	0.16	QJF77807.1
Octodon degus	Degu	0.14	XP_023575315.1
Trichechus manatus latirostris	Florida manatee	0.13	XP_004386381.1
Rhinolophus alcyone	Halcyon horseshoe bat	0.13	ALJ94035.1
Cavia porcellus	Domestic guinea pig	0.12	XP_023417808.1
Pipistrellus abramus	Japanese house bat	0.11	ACT66266.1
Theropithecus gelada	Gelada	0.10	XP_025218729.1
Chrysochloris asiatica	Cape golden mole	0.10	XP_006833624.1
Micronycteris hirsuta	Hairy big-eared bat	0.10	QJF77798.1

Continued

Species	Common name	Prediction scores	Data availability
Crocodylus porosus	Australian saltwater crocodile	0.09	XP_019384827.1
Crocodylus porosus	Australian saltwater crocodile	0.09	XP_019384826.1
Ornithorhynchus anatinus	Platypus	0.08	XP_001515597.2
Micronycteris microtis	Common big-eared bat	0.08	QJF77800.1
Chrysochloris asiatica	Cape golden mole	0.07	XP_006835673.1
Centronycteris centralis	Thomas's shaggy bat	0.07	QJF77790.1
Rhinolophus sinicus	Chinese rufous horseshoe bat	0.07	ADN93472.1
Balantiopteryx plicata	Gray sac-winged rat	0.03	QJF77825.1
Echinops telfairi	Small madagascar hedgehog	0.01	XP_004710002.1
Rhinolophus landeri	Lander's horseshoe bat	0.01	ALJ94034.1
Rhinolophus pusillus	Least horseshoe bat	0.01	ADN93477.1
Erinaceus europaeus	Western European hedgehog	0.00	XP_007538670.1
Saccopteryx bilineata	Greater sac-winged bat	0.00	QJF77808.1
Rhinolophus ferrumequinum	Greater horseshoe bat	0.00	BAH02663.1
Rhinolophus sinicus	Chinese rufous horseshoe bat	0.00	AGZ48803.1
Rhinolophus ferrumequinum	Greater horseshoe bat	0.00	ADN93470.1

Note: >0.5 prediction score in our analysis indicate bindiSilvery gibbon2 and SARS-CoV-2 spike.
Abbreviations: ACE2=angiotensin I converting enzyme 2; SARS-CoV-2=severe acute respiratory syndrome coronavirus 2.
* No common name.

SUPPLEMENTARY TABLE S4. Results of our predictions and the results of the experimental validation from Yan et al. (*8*).

Sequnece_name	Experiment results	Our prediction sore	Accession number
Rousettus_aegyptiacus	Binding	1.00	XM_016118926.1
Pteropus_alecto	Binding	1.00	XM_006911647.1
Pteropus_giganteus	Binding	1.00	GCA_902729225.1
Eidolon_helvum	Binding	1.00	GCA_000465285.1
Eonycteris_spelaea	Binding	1.00	GCA_003508835.1
Macroglossus_sobrinus	Binding	1.00	GCA_004027375.1
Cynopterus_sphinx	Not bind	0.93	MT515623
Cynopterus_brachyotis	Not bind	0.93	GCA_009793145.1
Rhinolophus_pearsonii	Not bind	0.09	MT515622
Hipposideros_armiger	Binding	0.70	XM_019667391.1
Hipposideros_galeritus	Not bind	0.72	GCA_004027415.1
Hipposideros_pratti	Not bind	0.70	MT515621
Megaderma_lyra	Binding	0.73	MT515624
Noctilio_leporinus	Binding	0.77	GCA_004026585.1
Taphozous_melanopogon	Binding	0.87	MT952961
Anoura_caudifer	Binding	0.72	GCA_004027475.1
Trachops_cirrhosus	Binding	0.26	MT952962
Vampyram_spectrum	Not bind	0.31	MT952963
Tonatia_saurophila	Not bind	0.14	GCA_004024845.1
Phyllostomus_discolor	Not bind	0.16	XM_028522516.1
Carollia_perspicillata	Binding	0.44	GCA_004027735.1
Micronycteris_hirsuta	Binding	0.11	GCA_004026765.1
Sturnira_hondurensis	Binding	0.44	GWHAAZA00000000
Artibeus_jamaicensis	Binding	0.93	GCA_004027435.1
Desmodus_rotundus	Binding	0.16	XM_024569930.1
Pteronotus_parnellii	Not bind	0.36	GCA_000465405.1
Mormoops_blainvillei	Binding	0.38	GCA_004026545.1
Pteronotus_davyi	Not bind	0.33	MT952964
Tadarida_brasiliensis	Not bind	0.37	GCA_004025005.1
Molossus_molossus	Not bind	0.49	https://vgp.github.io/genomeark/Molossus_molossus
Miniopterus_schreibersii	Binding	0.76	GCA_004026525.1
Miniopterus_natalensis	Not bind	0.22	GCA_001595765.1
Eptesicus_fuscus	Not bind	0.73	XM_008154928.2
Aeorestes_cinereus	Not bind	0.33	GCA_011751065.1
Pipistrellus_pipistrellus	Binding	0.36	GCA_004026625.1
Lasiurus_borealis	Not bind	0.29	GCA_004026805.1
Pipistrellus_kuhlii	Not bind	0.32	https://vgp.github.io/genomeark/Pipistrellus_kuhlii
Antrozous_pallidus	Binding	0.86	GCA_007922775.1
Nycticeius_humeralis	Not bind	0.47	GCA_007922795.1
Murina_feae	Not bind	0.48	GCA_004026665.1
Myotis_myotis	Binding	0.72	https://vgp.github.io/genomeark/Myotis_myotis
Myotis_davidii	Binding	0.79	XM_006775210.2
Myotis_brandtii	Binding	0.87	XM_014544294.1
Myotis_lucifugus	Binding	0.87	XM_023753669.1

Note: >0.5 prediction score in our analysis indicate binding between ACE2 and SARS-CoV-2 spike.
Abbreviations: ACE2=angiotensin I converting enzyme 2; SARS-CoV-2=severe acute respiratory syndrome coronavirus 2.

REFERENCES

1. Wang QH, Zhang YF, Wu LL, Niu S, Song CL, Zhang ZY, et al. Structural and functional basis of SARS-CoV-2 entry by using human ACE2. Cell 2020;181(4):894 – 904.e9. http://dx.doi.org/10.1016/j.cell.2020.03.045.
2. Liu YH, Hu GW, Wang YY, Ren WL, Zhao XM, Ji FS, et al. Functional and genetic analysis of viral receptor ACE2 orthologs reveals a broad potential host range of SARS-CoV-2. Proc Natl Acad Sci USA 2021;118(12):e2025373118. http://dx.doi.org/10.1073/pnas.2025373118.
3. Higgins DG, Sharp PM. CLUSTAL: a package for performing multiple sequence alignment on a microcomputer. Gene 1988;73(1):237 – 44. http://dx.doi.org/10.1016/0378-1119(88)90330-7.
4. Chan KK, Dorosky D, Sharma P, Abbasi SA, Dye JM, Kranz DM, et al. Engineering human ACE2 to optimize binding to the spike protein of SARS coronavirus 2. Science 2020;369(6508):1261 – 5. http://dx.doi.org/10.1126/science.abc0870.
5. Niu S, Wang J, Bai B, Wu LL, Zheng AQ, Chen Q, et al. Molecular basis of cross-species ACE2 interactions with SARS-CoV-2-like viruses of pangolin origin. EMBO J 2021;40(16):e107786. http://dx.doi.org/10.15252/embj.2021107786.
6. Letunic I, Bork P. Interactive tree of life (iTOL) v5: an online tool for phylogenetic tree display and annotation. Nucleic Acids Res 2021;49(W1):W293 – 6. http://dx.doi.org/10.1093/nar/gkab301.
7. Damas J, Hughes GM, Keough KC, Painter CA, Persky NS, Corbo M, et al. Broad host range of SARS-CoV-2 predicted by comparative and structural analysis of ACE2 in vertebrates. Proc Natl Acad Sci USA 2020;117(36):22311 – 22. http://dx.doi.org/10.1073/pnas.2010146117.
8. Yan H, Jiao HW, Liu QY, Zhang Z, Xiong Q, Wang BJ, et al. ACE2 receptor usage reveals variation in susceptibility to SARS-CoV and SARS-CoV-2 infection among bat species. Nat Ecol Evol 2021;5(5):600 – 8. http://dx.doi.org/10.1038/s41559-021-01407-1.

Methods and Applications

Field Validation of a Rapid Recombinase Aided Amplification Assay for SARS-CoV-2 RNA at Customs — Zhejiang Province, China, January 2021

Xinxin Shen[1,&]; Jinrong Wang[2,&]; Jingyi Li[1]; Anna He[1]; Hong Liu[3,#]; Xuejun Ma[1,4,#]

ABSTRACT

Introduction: The best approach to preventing the importation of coronavirus disease 2019 (COVID-19) is enhancing the detection capacity at customs. The rapid detection is of utmost importance and therefore highly demanded.

Methods: We conducted a field validation study of a duplex real-time reverse transcription recombinase-aided amplification (RT-RAA) assay in Zhoushan and Hangzhou customs, in Zhejiang Province, China. The reverse transcriptase polymerase chain reaction (RT-PCR) assay kit routinely used at customs was used in parallel, and the duration the two methods took to complete a specific number of samples was compared.

Results: Among 506 samples collected, RT-RAA results were consistent with the RT-PCR results. The sensitivity and specificity were 100%, the total coincidence rate was 100%, and the Kappa value was 1 (P<0.05) for both methods. The RT-RAA kit took a significantly shorter time in testing the 20–200 samples than the RT-PCR kit.

Discussion: The RT-RAA detection method is more efficient and suitable for use at customs than RT-PCR assay to realize rapid customs clearance of 200 or fewer samples.

INTRODUCTION

The coronavirus disease 2019 (COVID-19) pandemic has raised serious health and economic concerns worldwide (*1*). At present, China has effectively controlled the local spread of the disease. However, COVID-19 is still an active epidemic in many countries across the world (*2–3*). Therefore, preventing the importation of new COVID-19 strains from overseas and rebound of the domestic outbreaks are currently two major focus areas in China. The best approach to preventing the importation of COVID-19 from other countries is enhancing the detection capacity at customs where the detection accuracy and rapidity are highly demanded (*4*).

Reverse transcriptase polymerase chain reaction (RT-PCR) is a commonly used technique at customs for diagnosing COVID-19 (*5*). However, this method is time-consuming and requires specialized equipment and skilled personnel (*6*). The IgM or IgG-based assay has low sensitivity and requires a longer window period (*7–8*), making it unsuitable for early diagnosis, which is critical at customs. Previously, we conducted a multiple-center clinical evaluation of an ultrafast single-tube assay for severe acute respiratory syndrome coronavirus 2 (SARS-CoV-2) RNA. The method involved using a reverse transcription recombinase aided amplification (RT-RAA) assay. Notably, the detection was completed within 15 minutes at 39 °C using portable instruments after adding the extracted RNA samples (*9–10*). Our findings demonstrate that the RT-RAA assay has comparable sensitivity and specificity to the commercial RT-PCR kits and exhibits the distinctive advantages of simplicity and rapidity regarding operation and turnaround time. We validated the preceding RT-RAA assay by incorporating an internal control in the RAA system (*11*). The duplex RT-RAA kit was evaluated by the National Institutes for Food and Drug Control, China. According to the results, duplex RT-RAA kit had good specificity and the sensitivity of the duplex RT-RAA kit reached the range of 45 copies/mL to 137 copies/mL. Therefore, we conducted a field validation study at Zhoushan and Hangzhou customs, in Zhejiang Province, China. To evaluate the specificity and sensitivity of the RT-RAA kit, the PCR assay kit routinely used at customs was used in parallel, and the duration the two methods took to complete a specific number of samples was compared. This study provides reference data for establishing a rapid on-site detection of SARS-CoV-2 RNA at customs.

MATERIALS AND METHODS

Samples

A total of 506 nasopharyngeal swabs (273 samples in Hangzhou Customs and, 233 samples in Zhoushan Customs) were collected from visitors entering China between January 1, 2021, and January 25, 2021. The sample collection and preservation were performed according to the Guide of Laboratory Techniques for testing novel coronavirus infected pneumonia released by the National Health Commission of the People's Republic of China. After collection, the samples were inactivated at 56 °C for 30 min and stored at -80 °C. This study was approved by the institutional review committees of Hangzhou and Zhoushan Customs and was conducted as per the National Code of Ethics.

Nucleic Acid Extraction

Nucleic acid extraction was performed using the existing automated nucleic acid extractor that is routinely used at customs for detecting SARS-CoV-2 RNA. The specific nucleic acid extraction methods used at customs were summarized in Table 1. Total DNA/RNA was extracted from the samples using the methods outlined in Table 1, according to the manufacturers' instructions, and stored at -80 °C until use.

SARS-CoV-2 RNA was detected from the clinical samples using the COVID-19 RT-RAA kit, according to the methods described in our previous report (*10*–*11*). Positive controls (recombinant plasmids) and negative controls (DNase-free water) were included in each run to ensure the reliability of the experimental results. The 6-carboxy-fluoescein (FAM) channel was used to detect the amplification of the target gene, whereas the Hexachloro fluorescein (HEX) channel was used to detect the amplification of the internal control gene. The results were considered to be positive when both channels were positive or when the FAM channel was positive, and the HEX channel was negative. When the FAM channel was negative, but the HEX channel was positive, the result was negative. When both channels were negative, the result was considered invalid, and the RT-RAA assay was redone. The time it took to analyze specific numbers of samples using a particular method was recorded.

Analysis of Clinical Samples Using Reference RT-PCR Methods at Customs

Clinical samples were assessed for the presence of SARS-CoV-2 viral RNA using commercial COVID-19 quantitative RT-PCR kits (Easy Diagnosis Biomedicine Co, Wuhan, China, and DAAN GENE, Guangzhou, China in ZhouShan Customs, Easy Diagnosis Biomedicine Co, Wuhan, China and, BioGerm Medical Technology, Shanghai, China in Hangzhou Customs), according to the manufacturers' instructions. RT-PCR was performed alongside the RT-RAA kits at the facility sites (Hangzhou and Zhoushan Customs), where the clinical samples were stored. All the PCR procedures were performed on an ABI 7500 Real-Time PCR Instrument (Applied Biosystems, Foster City, CA) provided by the local customs. The time required to analyze a specific number of samples using a given method was recorded.

Comparing the Efficiency of RAA Versus RT-PCR for the Detection of SARS-CoV-2 RNA

The efficiencies of the COVID-19 nucleic acid detection kit (Fluorescence RT-RAA) and commercial RT-PCR nucleic acid detection kit were compared at the Hangzhou and Zhoushan customs. The parameters compared included the sensitivity, specificity, overall agreement rate, Kappa coefficient, and the time it took to complete 14, 28, 56, 98, and 196 samples using a specific method (*12*).

Statistical Data Analysis

IBM SPSS Statistics (version 21, IBM Corporation, NY, USA) was used to perform all the statistical

TABLE 1. Nucleic acid extraction methods used at the customs.

Manufacturer	Instrument model	Reagent	Extraction duration (min)	Institution
Tianlong	GeneRotex 96	Nucleic acid extraction kit	24	Hangzhou customs
Tianlong	NP968	Nucleic acid extraction kit	15	Zhoushan customs
Tiangen	TGuide S32	Total RNA extraction kit	18	Zhoushan customs
Bioperfectus	SSNP-2000A	Viral nucleic acid extraction kit	23	Zhoushan customs

Note: Detection of SARS-CoV-2 viral RNA in the clinical samples using RT-RAA kits.
Abbreviation: RT-RAA=real-time reverse transcription recombinase-aided amplification.

analysis. The results were analyzed using Kappa test and paired-samples t test, and a *P*-value less than 0.05 was considered statistically significant.

RESULTS

Analytical results of RAA were compared to those of RT-PCR for SARS-CoV-2 at Hangzhou Customs and Zhoushan Customs. Among the 506 samples collected by the Hangzhou customs and Zhoushan customs, 16 were positive, whereas 490 were negative as detected using the RT-RAA kit (Table 2). These results were consistent with the RT-PCR results. The sensitivity and specificity were 100%, the total coincidence rate was 100%, and the Kappa value was 1 ($P<0.05$) for both methods.

A time comparison was performed for the simultaneous detection of different numbers of specimens using RT-RAA and RT-PCR at Hangzhou Customs. The detection time of the RT-RAA kit was significantly shorter than that of the RT-PCR kit for samples less than 200, especially in the detection of samples <100 (Table 3).

DISCUSSION

The COVID-19 pandemic has seriously affected the physical and mental health of the world population. In addition, the pandemic situation has led to a significant reduction in economic development and social stability globally (*13*). Unfortunately, these circumstances are likely to persist for a long time before herd immunity can be achieved worldwide (*14*). As a forefront institution in the prevention of COVID-19 importation, China customs is still facing an enormous challenge, mainly because the rapid nucleic acid detection kits currently used are not suitable for SARS-CoV-2 on-site detection (*15*). Specifically, these kits are time-consuming and less sensitive. Therefore, there is an urgent need to develop more efficient techniques and products to fill in the deficiency of the existing ones.

Therefore, we demonstrate that the RT-RAA detection kit is accurate for detecting SARS-CoV-2 RNA in swab samples (*10*). This was verified by field testing of 506 samples (273 cases in Hangzhou customs and 233 cases in Zhoushan customs). Based on the testing results, the sensitivity and specificity of the RT-RAA detection kit was 100%, which was consistent with the results obtained using RT-PCR detection kits. Notably, the RAA detection reagents and equipment (RAA-B6100 and RAA-F1620) matched different nucleic acid extraction devices/reagents currently used at customs. The nucleic acid extractors used at customs include Tianlong GeneRotex 96, Tianlong NP968, Tiangen TGuide S32, and Bioperfectus SSNP-2000A.

The most distinctive features of the RT-RAA detection kit were its rapidity and flexibility. According to the results obtained after analyzing 20–200 samples, the RT-RAA kit was more efficient and took a significantly shorter time than the RT-PCR kit (for example, 22 min *vs*. 110 min for 14 samples, 112 min *vs*. 220 min for 98 samples). The RAA detection kit exhibits significant advantages over the RT-PCR kit, such as fast and flexible detection, and is, therefore, more suitable for use at customs clearance. Of note, it is mandatory to reanalyze clinical samples which turn positive after the initial test. In this case, the RT-RAA detection method is more applicable as it takes only 20 min compared to the RT-PCR method, which takes more than 90 min.

The limitations of current RT-RAA detection kit were the moderate throughput (16 samples one run) and requirement of nucleic acid extraction, which will be addressed in the future to better serve the customs. Nevertheless, this study showed that the RT-RAA detection method in its current format was efficient and suitable for use at customs as an alternative to RT-PCR assay. Therefore, we recommend that customs

TABLE 2. Results of SARS-CoV-2 analysis using RT-RAA versus RT-PCR detection kits (Hangzhou customs and Zhoushan customs).

Results obtained using RT-RAA nucleic acid detection kits	Results obtained using RT-PCR nucleic acid detection kits			Sensitivity (%)	Specificity (%)	Kappa	*P*
	Positive	Negative	Total				
Positive	16	0	16				
Negative	0	490	490	100	100	1	<0.05
Total	16	490	506				

Note: Time comparison of simultaneous detection of different numbers of specimens by RT-RAA and RT-PCR at Hangzhou customs.
Abbreviations: RT-RAA=real-time reverse transcription recombinase-aided amplification; RT-PCR=reverse transcriptase polymerase chain reaction.

TABLE 3. Comparison of the detection time between RT-RAA and RT-PCR detection kits.

Sample size (a)	14	28	56	98	196
Detection time (RT-RAA), minutes	22	37	67	112	202
Detection time (RT-PCR), minutes	110	110	110	220	330
P			<0.05		

Abbreviations: RT-RAA=real-time reverse transcription recombinase-aided amplification; RT-PCR=reverse transcriptase polymerase chain reaction.

adopt the RT-RAA detection method reported in the current study to realize rapid customs clearance of 200 or fewer samples. We anticipate that RT-RAA can be used to analyze 300 samples within 2 hours with more devices and personnel.

Conflicts of Interest: No conflict of interest declared.

Acknowledgements: Zhoushan and Hangzhou customs, Zhejiang Province, and Jiangsu Qitian Gene Biotechnology Co. Ltd.

Funding: Supported by grants from IVDC (2019HYDQNJJ03) and the key R & D projects in Zibo City (2020kj100011).

doi: 10.46234/ccdcw2021.236

[#] Corresponding authors: Hong Liu, liuhongseminar@hotmail.com; Xuejun Ma, maxj@ivdc.chinacdc.cn.

[1] National Institute for Viral Disease Control and Prevention, Chinese Center for Disease Control and Prevention, Beijing, China; [2] Shijiazhuang People's Hospital, Shijiazhuang, Hebei, China; [3] Shandong Provincial Research Center for Bioinformatic Engineering and Technique, School of Life Sciences and Medicine, Shandong University of Technology, Zibo, Shandong, China; [4] Center for Biosafety Mega-Science, Chinese Academy of Sciences, Wuhan, Hubei, China.

[&] Joint first authors.

Submitted: August 25, 2021; Accepted: October 22, 2021

REFERENCES

1. Sharma A, Ahmad Farouk I, Lal SK. COVID-19: a review on the novel coronavirus disease evolution, transmission, detection, control and prevention. Viruses 2021;13(2):202. http://dx.doi.org/10.3390/v13020202.
2. Salzberger B, Buder F, Lampl B, Ehrenstein B, Hitzenbichler F, Holzmann T, et al. Epidemiology of SARS-CoV-2. Infection 2021;49(2):233 – 9. http://dx.doi.org/10.1007/s15010-020-01531-3.
3. Atzrodt CL, Maknojia I, McCarthy RDP, Oldfield TM, Po J, Ta KTL, et al. A guide to COVID-19: a global pandemic caused by the novel coronavirus SARS-CoV-2. FEBS J 2020;287(17):3633 – 50. http://dx.doi.org/10.1111/febs.15375.
4. Read JM, Bridgen JRE, Cummings DAT, Ho A, Jewell CP. Novel coronavirus 2019-nCoV (COVID-19): early estimation of epidemiological parameters and epidemic size estimates. Philos Trans Roy Soc B Biol Sci 2021;376(1829):20200265. http://dx.doi.org/10.1098/rstb.2020.0265.
5. Wikramaratna PS, Paton RS, Ghafari M, Lourenço J. Estimating the false-negative test probability of SARS-CoV-2 by RT-PCR. Eurosurveillance 2020;25(50):2000568. http://dx.doi.org/10.2807/1560-7917.ES.2020.25.50.2000568.
6. Xue GH, Li SL, Zhang WW, Du B, Cui JH, Yan C, et al. Reverse-transcription recombinase-aided amplification assay for rapid detection of the 2019 novel coronavirus (SARS-CoV-2). Anal Chem 2020;92(14):9699 – 705. http://dx.doi.org/10.1021/acs.analchem.0c01032.
7. Padoan A, Cosma C, Sciacovelli L, Faggian D, Plebani M. Analytical performances of a chemiluminescence immunoassay for SARS-CoV-2 IgM/IgG and antibody kinetics. Clin Chem Lab Med 2020;58(7):1081 – 8. http://dx.doi.org/10.1515/cclm-2020-0443.
8. Safiabadi Tali SH, LeBlanc JJ, Sadiq Z, Oyewunmi OD, Camargo C, Nikpour B, et al. Tools and techniques for severe acute respiratory syndrome coronavirus 2 (SARS-CoV-2)/COVID-19 detection. Clin Microbiol Rev 2021;34(3):e00228 – 20. http://dx.doi.org/10.1128/CMR.00228-20.
9. Shahrajabian MH, Sun WL, Cheng Q. Different methods for molecular and rapid detection of human novel coronavirus. Curr Pharm Des 2021;27(25):2893 – 903. http://dx.doi.org/10.2174/1381612827666210604114411.
10. Wang J, Cai K, He X, Shen X, Wang J, Liu J, et al. Multiple-centre clinical evaluation of an ultrafast single-tube assay for SARS-CoV-2 RNA. Clin Microbiol Infect 2020;26(8):1076 – 81. http://dx.doi.org/10.1016/j.cmi.2020.05.007.
11. Zheng YZ, Chen JT, Li J, Wu XJ, Wen JZ, Liu XZ, et al. Reverse transcription recombinase-aided amplification assay with lateral flow dipstick assay for rapid detection of 2019 novel coronavirus. Front Cell Infect Microbiol 2021;11:1 – 7. http://dx.doi.org/10.3389/fcimb.2021.613304.
12. Wu T, Ge YY, Zhao KC, Zhu XJ, Chen Y, Wu B, et al. A reverse-transcription recombinase-aided amplification assay for the rapid detection of N gene of severe acute respiratory syndrome coronavirus 2(SARS-CoV-2). Virology 2020;549:1 – 4. http://dx.doi.org/10.1016/j.virol.2020.07.006.
13. Pan BH, Ji ZW, Sakkiah S, Guo WJ, Liu J, Patterson TA, et al. Identification of epidemiological traits by analysis of SARS–CoV–2 sequences. Viruses 2021;13(5):764. http://dx.doi.org/10.3390/v13050764.
14. Onyeaka H, Anumudu CK, Al-Sharify ZT, Egele-Godswill E, Mbaegbu P. COVID-19 pandemic: a review of the global lockdown and its far-reaching effects. Sci Prog 2021;104(2):368504211019854. http://dx.doi.org/10.1177/00368504211019854.
15. Yüce M, Filiztekin E, Özkaya KG. COVID-19 diagnosis -A review of current methods. Biosens Bioelectron 2021;172:112752. http://dx.doi.org/10.1016/j.bios.2020.112752.

Review

Epidemiology Features and Effectiveness of Vaccination and Non-Pharmaceutical Interventions of Delta and Lambda SARS-CoV-2 Variants

Wenqing Bai[1]; Yue Gu[1]; Haoliang Liu[2]; Lei Zhou[1,#]

As the epidemic time of COVID-19 outbreaks worldwide has extended and the range of prevalence has expanded, SARS-CoV-2 viruses have continuously evolved and mutated, and multiple virus variants have successively emerged. Recently, the Delta and Lambda variants have attracted considerable attention in China for their transmissibility, infective incubation period, and pathogenicity. In this review, we describe the epidemic characteristics and prevention and control measures for Delta and Lambda.

The coronavirus disease 2019 (COVID-19), which was discovered in Wuhan in late December 2019, is an acute respiratory infectious disease caused by severe acute respiratory syndrome coronavirus 2 (SARS-CoV-2) (*1*–*4*). On March 13, 2020, the World Health Organization (WHO) declared COVID-19 as a global pandemic (*5*). As of September 21, 2021, more than 228 million people have been infected globally and nearly 4.6 million people have died (*6*).

As the COVID-19 pandemic continued and spread more widely, a variety of SARS-CoV-2 variants have emerged. These variants have the characteristics of faster replication and transmission, higher pathogenicity and potential immune escape, which led to a rebound of the epidemic recently (*7*). The WHO has classified several variants into variants of concern (VOC) and variant of interest (VOI) based on differences in transmissibility and pathogenicity, and the rest of the descendent lineages are designated as variants under monitoring (*8*). Currently, there are four VOCs, among which, the Delta variant has gradually become the dominant strain in many countries. The recent domestic outbreaks in China associated with the imported cases were mainly caused by the Delta variant (*9*–*10*). Among the two VOIs, the Lambda variant has recently appeared in South America and even in a few countries, and had a tendency to replace the Delta variant as the dominant strain (*11*).

Currently, four types of COVID-19 vaccines are available globally, including mRNA-1273 (Moderna INC., USA), BNT162b2 mRNA (Pfizer, New York, USA), AZD1222 (Oxford/AstraZeneca, UK), Janssen Ad26.CoV2.S (Johnson & Johnson, New Jersey, USA), etc. (*12*). Four types of COVID-19 vaccines including BBIBP-CorV (Sinopharm, Shanghai, China), WIBP-CorV (Sinopharm, Shanghai, China), Ad5-nCoV (CanSinoBIO, Tianjin, China), and CoronaVac (Sinovac Biotech, Beijing, China) have been approved in China (*13*). As of September 21, 2021, 2.48 billion people worldwide have completed the whole course of vaccination, of which, the top 3 countries are China, European Union, USA, and China ranked the first at 1,022 million people (*14*). The effect of vaccination on the SARS-CoV-2 virus, especially the current predominant strain of Delta variant, has become the focus of global concern.

Non-pharmaceutical interventions (NPIs) primarily refer to effective measures that can be taken to slow the spread of a virus in the absence of a safe and effective vaccine, treatment, or other prophylactic measures (*15*). Evidence has shown that social distancing, personal hygiene, mask wearing, case isolation, schools and businesses closure, transportation banning, gatherings cancelation, and other NPIs have played an important role in stopping the virus transmission and depressing the peak of the epidemic during the first COVID-19 event in Wuhan, China (*15*–*16*). However, the dominant SARS-CoV-2 strain has mutated significantly since, raising questions of what are the differences between the variants and whether the NPIs are still effective for the variants, especially the current predominant Delta variant and the emergent Lambda variant.

To be prepared in advance and to provide a basis for the control of infection (*17*), the pathogenicity, prevalence, transmissibility of Delta and Lambda variants, as well as the efficacy of vaccine and NPIs are reviewed in this article.

DELTA VARIANT

The Delta (B.1.617.2) variant was first identified in October 2020 in Maharashtra, India and was classified as a VOC in May 2021 by WHO. As of July 29, 2021, the Delta variant has been reported in at least 132 countries/territories and become a predominant strain in many countries.

Pathogenicity

The Delta variant contains 10 mutation sites in the spike glycoprotein (*18*), including 3 essential mutations, L452R, E484Q, and D614G (*19*). The L452R mutation is located in the S1 region of the spike glycoprotein, which has a receptor binding domain (RBD) that binds directly to the ACE2 receptor and is also a major target of anti-SARS-CoV-2 neutralizing antibodies (*20*). The L452R mutation has been shown to increase the infectivity of Delta variant and enhance the ability of neutralization escape (*17*). The P681R mutation, located near the S1/S2 cleavage site of the S-protein, promotes the cleavage of the S-protein, which also increases the infectivity of the Delta variant and completely blocks antibody recognition (*21*). In addition, several studies have found that the T478K mutation enhances the ability of the virus to bind to humans (*17*).

To date, the Delta variant has been further derived as the Delta plus variant or later named AY.1 variant. The AY variants included AY.4–AY.11 in the United Kingdom, AY.12 in Israel, AY.23 in Singapore and Indonesia, and AY.25 circulated in North America (*22*). This Delta plus variant contains an additional K417N S-protein mutation compared to the original Delta variant, which was also found in the Beta and Gamma variants. Some reports indicated that the Delta plus variant was more infectious and pathogenic than the original Delta variant (*23*).

Epidemiological Features

The first case infected with the Delta variant was identified in the UK in mid-April 2021 and then the Delta variant strain triggered the third wave of SARS-CoV-2 epidemic in the country, forcing the government of the UK to postpone the full reopening till June 21 (*17*). Besides the UK, the cases infected with Delta variant steadily increased in Denmark and the Delta variant became the dominant strain (*24*). In United States, according to a nationwide sampling survey, the proportion of the Alpha variant, the original strain of the virus, decreased from over 70% in late April down to about 42% in mid-June 2021, indicating that the Delta variant had been already dominating (*25*). In Africa, cases infected with the Delta variant were reported in Congo, Malawi, Uganda, and South Africa, raising concerns that the Delta variant will cause a surge of cases in African countries due to the limited access to vaccines and will pose the greatest risk to Africa (*24*).

For the Delta plus variants, according to the REGENERON, a Global Initiative on Sharing All Influenza Data (GISAID)-related online virus statistic database, more than 70% of the cases currently in Israel were infected with a Delta plus variant, including AY.12 which was about 59% currently prevalent and AY.4, AY.5, AY.6, and AY.9. The proportion of all cases infected with Delta plus variants in Latin America (AY.12 and AY.4), Singapore (AY.23), and Indonesia is accounted for 38%, 98%, and 71%, respectively (*11*).

Infectivity and Transmissibility

The high infectivity and viral load of the Delta variant has contributed to the continuity of the global COVID-19 pandemic. Studies in the UK indicated that the risk of hospitalization and infectiousness of Delta variant was 100% and 60%, respectively, more than the Alpha variant strain and that the Delta variant could infect 5 to 9 persons, more than the prototype strain that was isolated in Wuhan (2 to 3 persons) (*24*). In the Guangzhou outbreak caused by the Delta variant, compared with the other SARS-CoV-2 virus, the incubation period of the first-, second-, and third-generations of cases was 4, 5 to 6, and 10 days, respectively, which was shortened by 5 days, and the days from exposure to becoming infectious was significantly lower by roughly 2 to 4 days (*26*). Individuals infected with Delta variant could develop typical clinical symptoms 2 to 3 days after infection and could cause five generations of cases within 10 days with a R_0 of 4.04 to 5.0, which was much higher than that of the prototype strain that was isolated in Wuhan (2.2 to 3.77) (*17*).

Evidence indicated that the transmission routes of SARS-CoV-2 included respiratory droplets, fomites, and aerosol (*27–28*). The risk of spread of the Delta variant increased through aerosol transmission. Three separate incidents, including five cases associated with playing squash at a sports venue in Maribor, Slovenia (*29*), a cluster of cases associated with a shopping mall in Wenzhou, China (*30*), and an outbreak occurred in

the rehearsal of Skagit Valley Hymn in West Virginia, USA (*31*), indicated potential aerosol transmission of the Delta variant. The index case of recent domestic outbreak in Guangzhou was infected in the hospital where the imported case was isolated and tested, which was later determined to be where the aerosol transmission very likely occurred (*32*).

Vaccine Effect

One of the important measures to prevent severe illness and death is vaccination, but the effectiveness of vaccines has been weakened by the Delta variant and breakthrough infections have been reported continuously. A study found that Delta variant has a two-fold reduction in neutralizing titers compared to the other prior strains one month after vaccination with Pfizer (*33*). Overall, 71 of 218 Delta variant infections at the 5 study sites met the definition of vaccine breakthrough in a Singaporean study (*34*). A study from the UK found that the 6 types of neutralization antibodies of the Delta variant in sera collected from AstraZeneca and Pfizer vaccine recipients reduced more than 5-fold (*35*). Another UK study found that a single dose of either the AstraZeneca or Pfizer vaccine could reduce risk of individual infection with the Delta variant by 33%, which was lower than that with the Alpha variant (50%). Furthermore, 2 doses of the AstraZeneca vaccination could increase protection efficacy against Delta variant by 60%, which was lower than that against the Alpha variant (66%); meanwhile, 2 doses of Pfizer's vaccination could increase 88% prevention effectiveness to the Delta variant in comparison with 93% of Alpha variant (*24*,*36*). A study in Israel showed a 2.5-fold reduction in neutralization titers for Delta variants, while, a 1.7-fold, 10-fold, and 2-fold reduction in Alpha, Beta, and Gamma variants, respectively, between 4 and 14 days after the uptake of the second dose of Pfizer vaccine, resulting in an only 39% protection rate against symptomatic infection with Delta variant (*22*). US CDC reported a 66% protection rate after vaccination against Delta variant infection, which was considered a slight decrease following the continuous vaccination campaign (*37*). Another study in a nursing home in the United States reported a significant decrease in the effectiveness of the mRNA vaccine to prevent infection with Delta variant from 74.7% before the Delta variant emerged between March 1 to May 9, 2021, down to 53.1% after Delta variant dominated in the country (*38*). The recent outbreak in Guangdong revealed that the inactivated vaccine developed in China has a relevant high effectiveness to Delta variant including a 69% prevention of infection and more than 95% effectiveness of severe disease (*17*). The Phase III clinical data of Jiffy recombinant COVID-19 vaccine indicated that the total protection efficiency was 82% and the protection rate against Delta variant was 78% (*19*).

LAMBDA VARIANT

Although the Lambda variant has not been spreading as fast as Delta variant, the Lambda variant has been widely spread in South America and reported from over 35 countries/regions since it was first identified in Peru, where the case-fatality ratio has reached as high as 596 per 100,000 people (*39*).

Pathogenicity

The Lambda variant belongs to the C.37 lineage and classified as a VOI on June 14, 2021 by the WHO. The mutations in the domain of RBD and N-terminal domain (NTD) of the SARS-CoV-2 S protein can lead to the immune evasion because RBD and NTD are associated with the escape neutralization (*40*). A study published on BioRxiv preprint showed that the unique 7-amino-acid deletion of the RSYLTPGD246-253N mutation in the NTD of Lambda S protein resulted in its escape from neutralizing antibodies, which was the cause of the rapid spread of the Lambda variant in the Southern American countries (*41*). In addition, the T76I and L452Q mutations of Lambda variant can make the virus highly infectious (*34*) .

Epidemiological Features

In the past two months, The Lambda variant has been predominant in Peru, Chile, Argentina, Colombia, Uruguay, Paraguay, and other South American countries (*23*), According to the GISAID database, since the first case of Lambda variant was reported in the United States on July 22, 2021, 1,060 cases infection with Lambda variant have been reported, and later, Lambda variant has spread from America to Asia (*42*). On August 6, a 30-year-old woman arrived at Tokyo Haneda Airport from Peru and was diagnosed with Lambda variant infection, who was the first case of Lambda variant in Japan.

Although the impact of Lambda variant in Peru is increasing, the number of cases of Lambda variant in other countries has not yet exceeded that of Delta

variant. The proportion of Lambda variant in the UK and United States is less than 0.1% and 0.3%, respectively. To explain the inconsistent performance of Lambda variant in different countries/regions, the "founder effect" which means that the predominant variant is usually firstly introduced and spread in a densely and restricted population, might be an important factor (*42*).

Vaccine Effect

Similar with the Delta variant, partial mutations of the Lambda variant cause the virus to escape neutralizing antibodies, but a small amount of mutations may not be enough to make the Lambda variant completely escape from the immune system, even unusual mutations due to T cell function. In comparison with the D614G mutation, the L452Q mutation of the Lambda variant increases its ability to bind to cells by 2-fold and the L452Q and F490S mutations increased the serum resistance of convalescent patients by 3.3-fold, which was lower than Beta variant (4.9-fold), the study also found that the serum resistance of Lambda variant to Pfizer and Moderna vaccine increased by 3- and 2.3-fold, respectively, but the mRNA vaccines such as Pfizer and Moderna remained effective for Lambda variants (*43*). Similarly, a study of the impact of the CoronaVac vaccine on the Lambda variant found that neutralizing antibodies had only 3.05-fold less than the prior variant (*44*), indicating that part of the neutralizing antibody was retained.

THE CONTROL AND PREVENTION MEASURES

The global COVID-19 pandemic is still ongoing, and the viruses continue to adapt, changing their characteristics such as the infectivity, transmissibility, and pathogenicity. On August 30, 2021, the WHO announced the Mu variant (B.1.621) and classified it as a VOI (*8*,*45*), which has mutations associated with potential immune escape. More studies of the phenotypic and clinical characteristics of Mu variant, and the monitoring of any changes with the co-circulation of the Delta, Lambda, and the other variants are needed (*45*–*46*).

The emerging SARS-CoV-2 variants pose great challenges to the prevention and control of epidemics. The WHO recommends that ongoing pandemic prevention strategies and measures will continue to work on variants (*8*). The Chinese experiences illustrated that vaccination alone cannot block infection and transmission due to the ultra-short incubation period (*19*). To prevent and control the transmission of Delta and Lambda variants, China continues to adopt proactive strategies and implement a series of NPIs (*21*,*45*,*47*–*48*) .

In addition, the research on Delta and Lambda variants should be further promoted, especially on the mutation sites related with immune recognition and vaccine efficacy (*49*). The WHO encourages countries to strengthen gene monitoring and viral sequencing capabilities and calls for close cooperation among countries to strengthen the monitoring of variation and the evaluation of biological characteristics of variants, which needs timely sharing of the information to early alert the potential important immune escape variants (*8*,*42*).

Funding: This work was supported by the National Natural Science Foundation (grant number 71934002) of the People's Republic of China.

doi: 10.46234/ccdcw2021.216

[#] Corresponding author: Lei Zhou, zhoulei@chinacdc.cn.

[1] Chinese Center for Disease Control and Prevention, Beijing, China; [2] Nanjing Medical University, Nanjing, Jiangsu, China.

Submitted: September 18, 2021; Accepted: October 04, 2021

REFERENCES

1. Wu F, Zhao S, Yu B, Chen YM, Wang W, Song ZG, et al. A new coronavirus associated with human respiratory disease in China. Nature 2020;579(7798):265 – 9. http://dx.doi.org/10.1038/s41586-020-2008-3.
2. Zhou P, Yang XL, Wang XG, Hu B, Zhang L, Zhang W, et al. A pneumonia outbreak associated with a new coronavirus of probable bat origin. Nature 2020;579(7798):270 – 3. http://dx.doi.org/10.1038/s41586-020-2012-7.
3. Zhu N, Zhang DY, Wang WL, Li XW, Yang B, Song JD, et al. A novel coronavirus from patients with pneumonia in China, 2019. N Engl J Med 2020;382(8):727 – 33. http://dx.doi.org/10.1056/NEJMoa2001017.
4. Li Q, Guan XH, Wu P, Wang XY, Zhou L, Tong YQ, et al. Early transmission dynamics in Wuhan, China, of novel coronavirus-infected pneumonia. N Engl J Med 2020;382(13):1199 – 207. http://dx.doi.org/10.1056/NEJMoa2001316.
5. World Health Organization. WHO Director-General's opening remarks at the media briefing on COVID-19 - 11 March 2020. 2020. https://www.who.int/director-general/speeches/detail/who-director-general-s-opening-remarks-at-the-media-briefing-on-covid-19---11-march-2020. [2021-9-4].
6. World Health Organization. WHO coronavirus (COVID-19) dashboard. 2021. https://covid19.who.int/. [2021-9-4].
7. Lauring AS, Hodcroft EB. Genetic variants of SARS-CoV-2-what do they mean? JAMA 2021;325(6):529 – 31. http://dx.doi.org/10.1001/jama.2020.27124.
8. World Health Organization. Tracking SARS-CoV-2 variants. 2021.

https://www.who.int/en/activities/tracking-SARS-CoV-2-variants/. [2021-9-22].
9. Wang FZ, An ZJ, Rodewald L, Wu D, Tang L, Zheng H, et al. Guangdong's study of the effectiveness of China's inactivated vaccines against the SARS-CoV-2 B. 1. 617. 2 (Delta) variant.. China CDC Wkly 2021;3(34):728 – 30. http://dx.doi.org/10.46234/ccdcw2021.179.
10. Chadha J, Khullar L, Mittal N. Facing the wrath of enigmatic mutations: a review on the emergence of severe acute respiratory syndrome coronavirus 2 variants amid coronavirus disease-19 pandemic. Environ Microbiol 2021. http://dx. doi.org/10.1111/1462-2920.15687.
11. REGENERON. COVID-19 dashboard. 2021. https://covid19dashboard.regeneron.com/?tab=Variant_Graphs&subTab=Top_Variants_Over_Time_(Select_Location). [2021-8-24].
12. World Health Organization. WHO recommendation COVID-19 vaccine BIBP/sinopharm. 2021. https://extranet.who.int/pqweb/vaccines/who-recommendation-covid-19-vaccine-bibp. [2021-9-4].
13. World Health Organization. Status of COVID-19 Vaccines within WHO EUL/PQ evaluation process. 2021. https://extranet.who.int/pqweb/sites/default/files/documents/Status_COVID_VAX_20Jan2021.pdf.
14. Our World in Data. Coronavirus (COVID-19) vaccinations. 2021. https://ourworldindata.org/covid-vaccinations. [2021-9-22].
15. Melnick ER, Ioannidis JPA. Should governments continue lockdown to slow the spread of covid-19? BMJ 2020;369:m1924. http://dx.doi.org/10.1136/bmj.m1924.
16. Li C, Zhong Y, Wu Y, Yang CH, Zhou LJ,Zhang T. Research and prospect of non-pharmaceutical interventions in COVID-19. Mod Prev Med 2021;48(3):385 – 8.
17. Shi QF, Gao XD, Hu BJ. Research progress on characteristics, epidemiology and control measure of SARS-CoV-2 Delta VOC. Chin J Nosocomiol 2021. http://kns.cnki.net/kcms/detail/11.3456.R.20210707.2126.070.html. [2021-9-16]. (In Chinese).
18. Cascella M, Rajnik M, Aleem A, Dulebohn SC, Di Napoli R. Features, evaluation, and treatment of coronavirus (COVID-19). In: StatPearls [Internet]. Treasure Island (FL): StatPearls Publishing. 2021. https://pubmed.ncbi.nlm.nih.gov/32150360/.
19. Zhao X, Zheng AQ, Li DD, Zhang R, Sun H, Wang QH, et al. Neutralization of recombinant RBD-subunit vaccine ZF2001-elicited antisera to SARS-CoV-2 variants including Delta. bioRxiv 2021. http://dx. doi.org/10.1101/2021.07.15.452504.
20. Khateeb J, Li YC, Zhang HB. Emerging SARS-CoV-2 variants of concern and potential intervention approaches. Crit Care 2021;25(1):244. http://dx.doi.org/10.1186/s13054-021-03662-x.
21. Feng YN, Song Y, Wang SW, Chen C, Xu WB. Research advances in global SARS-CoV-2 variants. Chin J Virol 2021;37(3):17. (In Chinese).
22. Pango Network. New AY lineages. 2021. https://www.pango.network/new-ay-lineages/. [2021-9-14].
23. Kannan SR, Spratt AN, Cohen AR, Naqvi SH, Chand HS, Quinn TP, et al. Evolutionary analysis of the Delta and Delta Plus variants of the SARS-CoV-2 viruses. J Autoimmun 2021;124:102715. http://dx.doi.org/10.1016/j.jaut.2021.102715.
24. Callaway E. Delta coronavirus variant: scientists brace for impact. Nature 2021;595(7865):17 – 8. http://dx.doi.org/10.1038/d41586-021-01696-3.
25. Bolze A, Cirulli ET, Luo SS, White S, Wyman D, Dei Rossi A, et al. SARS-CoV-2 variant Delta rapidly displaced variant Alpha in the United States and led to higher viral loads. medRxiv 2021. http://dx.doi.org/10.1101/2021.06.20.21259195.
26. Zhuo JT. The strategy to overcome attack with an ultra-short incubation period and escape with an ultra-long incubation period of the COVID-19 Delta variant of based on cases of outbreaks and their containment. Shanghai J Prev Med 2021. http://kns.cnki.net/kcms/detail/31.1635.R.20210729.1041.002.html. [2021-9-16]. (In Chinese).
27. Tang S, Mao YX, Jones RM, Tan QY, Ji JS, Li N, et al. Aerosol transmission of SARS-CoV-2? Evidence, prevention and control. Environ Int 2020;144:106039. http://dx.doi.org/10.1016/j.envint.2020.106039.
28. Jones RM, Brosseau LM. Aerosol transmission of infectious disease. J Occup Environ Med 2015;57(5):501 – 8. http://dx.doi.org/10.1097/JOM.0000000000000448.
29. Brlek A, Vidovič Š, Vuzem S, Turk K, Simonović Z. Possible indirect transmission of COVID-19 at a squash court, Slovenia, March 2020: case report. Epidemiol Infect 2020;148:e120. http://dx.doi.org/10.1017/S0950268820001326.
30. Cai J, Sun WJ, Huang JP, Gamber M, Wu J, He GQ. Indirect virus transmission in cluster of COVID-19 cases, Wenzhou, China, 2020. Emerg Infect Dis 2020;26(6):1343 – 5. http://dx.doi.org/10.3201/eid2606.200412.
31. Miller SL, Nazaroff WW, Jimenez JL, Boerstra A, Buonanno G, Dancer SJ, et al. Transmission of SARS-CoV-2 by inhalation of respiratory aerosol in the Skagit Valley Chorale superspreading event. Indoor Air 2021;31(2):314 – 23. http://dx.doi.org/10.1111/ina.12751.
32. Zhang ZN, Li X, Wang Q, Xu J, Jiang QQ, Jiang SL, et al. Field simulation of aerosol transmission of SARS-CoV-2 in a special building layout — Guangdong province, China, 2021. China CDC Wkly 2021;3(34):711 – 5. http://dx.doi.org/10.46234/ccdcw2021.176.
33. Lustig Y, Zuckerman N, Nemet I, Atari N, Kliker L, Regev-Yochay G, et al. Neutralising capacity against Delta (B. 1. 617. 2) and other variants of concern following Comirnaty (BNT162b2, BioNTech/Pfizer) vaccination in health care workers, Israel. Eurosurveillance 2021;26(26):pii=2100557. http://dx.doi.org/10.2807/1560-7917.ES.2021.26.26.2100557.
34. Chia PY, Ong SWX, Chiew CJ, Ang LW, Chavatte JM, Mak TM, et al. Virological and serological kinetics of SARS-CoV-2 Delta variant vaccine-breakthrough infections: a multi-center cohort study. medRxiv 2021. http://dx. doi.org/10.1101/2021.07.28.21261295.
35. Liu C, Ginn HM, Dejnirattisai W, Supasa P, Wang BB, Tuekprakhon A, et al. Reduced neutralization of SARS-CoV-2 B. 1. 617 by vaccine and convalescent serum. Cell 2021;184(16):4220 – 36.e13. http://dx.doi.org/10.1016/j.cell.2021.06.020.
36. Farinholt T, Doddapaneni H, Qin X, Menon V, Meng QC, Metcalf G, et al. Transmission event of SARS-CoV-2 Delta variant reveals multiple vaccine breakthrough infections. medRxiv 2021. http://dx.doi.org/10.1101/2021.06.28.21258780.
37. Fowlkes A, Gaglani M, Groover K, Thiese MS, Tyner H, Ellingson K, et al. Effectiveness of COVID-19 vaccines in preventing SARS-CoV-2 infection among frontline workers before and during B. 1. 617. 2 (Delta) variant predominance - eight U. S. locations, December 2020(34):1167 – 9. http://dx.doi.org/10.15585/mmwr.mm7034e4.
38. Nanduri S, Pilishvili T, Derado G, Soe MM, Dollard P, Wu H, et al. Effectiveness of pfizer-BioNTech and moderna vaccines in preventing SARS-CoV-2 infection among nursing home residents before and during widespread circulation of the SARS-CoV-2 B. 1. 617. 2 (Delta) variant - national healthcare safety network, March 1-August 1, 2021(34):1163 – 6. http://dx.doi.org/10.15585/mmwr.mm7034e3.
39. Coronavirus (COVID-19) Deaths- Statistics and Research - Our World in Data[EB/OL]. [2021/9/21]. https://ourworldindata.org/covid-deaths.
40. Bose P. Scientists suspect Lambda SARS-CoV-2 variant most dangerous. News-Medical. 2021. https://www.news-medical.net/news/20210730/Scientists-suspect-Lambda-SARS-CoV-2-variant-most-dangerous.aspx. [2021-9-16].
41. Kimura I, Kosugi Y, Wu JQ, Yamasoba D, Butlertanaka EP, Tanaka YL, et al. SARS-CoV-2 Lambda variant exhibits higher infectivity and immune resistance. bioRxiv 2021. http://dx.doi.org/10.1101/2021.07.28.454085.
42. Sina Finance. Variants of the SARS-CoV-2 viruses emerge in endlessly, and "Lamda" appears after "Delta". 2021. https://baijiahao.baidu.com/s?id=1707407314247784486&wfr=spider&for=pc. [2021-8-19]. (In Chinese).
43. Tada T, Zhou H, Dcosta BM, Samanovic MI, Mulligan MJ, Landau NR. SARS-CoV-2 lambda variant remains susceptible to neutralization

by mRNA vaccine-elicited antibodies and convalescent serum. bioRxiv 2021. http://dx. doi.org/10.1101/2021.07.02.450959.
44. Acevedo ML, Alonso-Palomares L, Bustamante A, Gaggero A, Paredes F, Cortés CP, et al. Infectivity and immune escape of the new SARS-CoV-2 variant of interest Lambda. medRxiv 2021. http://dx.doi.org/10.1101/2021.06.28.21259673.
45. National Health Commission of the People's Republic of China. Notice on issuing the normalization of prevention and control guidelines f COVID-19 (August 2021) for focus populations in focus units and units. 2021. http://www.nhc.gov.cn/xcs/zhengcwj/202108/ead4082ee97b49a38a8512e112f53dbf.shtml. [2021-9-4]. (In Chinese).
46. World Health Organization. Weekly epidemiological update on COVID-19 - 31 August 2021. 2021. http://www.gov.cn/xinwen/2020-04/09/content_5500689.htm. [2021-9-6].
47. National Health Commission of the People's Republic of China. Notice on issuing the guidelines for the public and focus occupational groups to wear masks (August 2021 Edition). 2021. http://www.gov.cn/xinwen/2021-08/13/content_5631097.htm. [2021-9-4]. (In Chinese).
48. National Health Commission of the People's Republic of China. Notice on issuing the protocol for prevention and control of COVID-19 (Edition 8). 2021. http://www.gov.cn/xinwen/2021-05/14/content_5606469.htm. [2021-9-4]. (In Chinese).
49. Yang TH, Zhang XY, Xu JQ. SARS-CoV-2 vaccines: current situation and prospect. Chin J Infect Control 2021;20(7): 673–80. http://www.zggrkz.com/CN/abstract/abstract30922.shtml. (In Chinese).

Notes from the Field

Two Cases of COVID-19 with Persistently Positive SARS-CoV-2-Specific IgM During One-Year Follow-Up — Sichuan Province, China, February 2021

Bennan Zhao[1,2,&]; Yuezhu Chen[1,&]; Yong Yue[3,&]; Dafeng Liu[2]; Guihui Wu[2]; Yi Mao[2]; Liang Wang[3]; Zhu Liu[1,3,#]

On January 22, 2020, a 41-year-old male (Patient A) developed a fever with a maximum temperature of 38 °C after returning to Chengdu City from Wuhan City. He was admitted to the Public Health Clinical Center of Chengdu on January 26, 2020, after being confirmed to be positive for coronavirus disease 2019 (COVID-19) by Chengdu CDC. Chest computed tomography (CT) revealed multiple plaque-like, ground-glass shadows in the upper, middle, and lower lobes of the right lung and upper and lower lobes of the left lung, as well as a small amount of pericardial effusion.

On January 23, 2020, a 45-year-old female (Patient B) developed shortness of breath and muscle soreness, along with decreased muscle strength after returning from Japan. After 5 days, she experienced a fever (T_{max}=38.3 °C) and was admitted to Sichuan Provincial People's Hospital for treatment. She tested positive for COVID-19 by Chengdu CDC on January 29, 2020. Chest CT revealed plaque-like, ground-glass density shadows and nodular shadows in multiple lobes and segments, especially in the upper lobes of both lungs. About half a month later, another chest CT showed a small amount of pericardial effusion.

Patients A and B were categorized as common-type cases of COVID-19 according to the Diagnosis and Treatment Protocol for COVID-19 (Trial Version 5) (*1*). Laboratory tests on admission showed that the lymphocyte count, platelet count, $CD4^+$ T-cell count, and $CD8^+$ T-cell count of Patient A were below the normal range. In Patient B, only the $CD8^+$ T-cell count was below the normal range. During follow-up, the platelet counts of Patient A were always below the normal range (100×10^9/L–300×10^9/L); the lowest level was 32×10^9/L, and the most recent result was 75×10^9/L. At the hospital, Patient B was identified as possibly having anxiety as her most recent Depression, Anxiety, and Stress Scale-21 Items (DASS-21) total score reached 23. In both patients, pericardial effusions were observed in chest radiology images, suggesting a possibility of pericarditis. In addition, cardiac magnetic resonance imaging (MRI) indicated myocardial microcirculation injury. The physical and mental health of both patients were affected.

As of February 9, 2021, Patients A and B have been followed-up with 7 times within a year (Figure 1). Both patients tested positive for COVID-19 using nucleic acid tests at their first follow-up visit about half a month after discharge and were immediately readmitted to the hospital. After the second discharge from the hospital, both patients continued to participate in regular follow-ups, and their nucleic acid tests remained negative. However, their SARS-CoV-2-specific IgM remained positive from the fourth follow-up visit (approximately four months after the onset of symptoms) up to the latest follow-up visit (about a year after the onset of symptoms).

IgM typically appears in the early stage and has a rather short maintenance time, so IgM is often used as an indicator for diagnosis and infection. In a study in Spain, the estimated duration of the persistence of IgM was 1.95 months, which was much shorter than the duration in our cases (*2*). In this study, SARS-CoV-2-specific IgM was detected using chemiluminescence immunoassay (CLIA) with the i 3000 Automatic Chemiluminescence Immunoassay Analyzer (Maccura Biotechnology Co.) and the SARS-CoV-2 IgM Detection Kit (Maccura Biotechnology Co.). Among all 34 patients who were followed-up with for one year, only Patients A and B presented with persistently positive IgM. Both Patients A and B met the discharge standard but had a recurrence of positive nucleic acid test results at the first follow-up visit, and their SARS-CoV-2-specific IgM remained positive for more than 8 months. In a cross-sectional study in Wuhan, 1.5% of respondents with SARS-CoV-2 infection also presented with positive IgM at approximately 9 months after infection (*3*).

In general, persistently positive IgM results are associated with reinfection or recurrence. In this case, there was little possibility for reinfection as these patients had no close contact with other patients infected with COVID-19 during hospitalization and

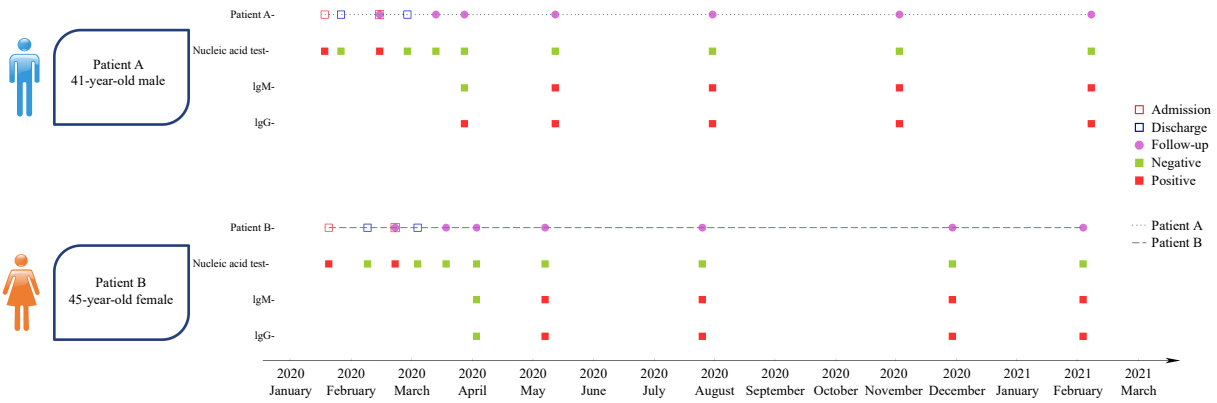

FIGURE 1. The timeline of admission, discharge, follow-up visits, and diagnostic testing for Patients A and B — China, 2020–2021.

rehabilitation. In addition, Patients A and B did not have additional recurrences since the second follow-up visit. This phenomenon may have indicated that the virus in their body was not completely eliminated. It was possible that the viral replication was maintained at a low level so that viral load was below the limit of detection. A recent study indicated that declining IgM may be a sign of virus clearance (*4*), which is consistent with our speculation. Despite the fact that both patients were non-severe COVID-19 cases, their $CD4^+$ T-cell count and/or $CD8^+$ T-cell count were below the normal range during hospitalization and had no sign of significant increase during rehabilitation, even though both patients received treatment for immunomodulation. For most COVID-19 patients, including those who went through regular follow-up visits in the Public Health Clinical Center of Chengdu, $CD4^+$ T-cell and $CD8^+$ T-cell levels increased over time. Therefore, Patients A and B most likely had suppressed and/or dysregulated immune system activity as their immune systems may have taken longer to eliminate the virus completely. The remaining virus can stimulate the body to produce antibodies, leading to persistently positive SARS-CoV-2-specific IgM.

Even though Patients A and B did not have additional recurrences since the second follow-up visit, the results showing persistently positive SARS-CoV-2-specific IgM may indicate the presence of virus and a possibility of long-term, intermittent virus shedding. This suggested that patients with persistently positive IgM results still have a risk of transmission. In this situation, close follow-ups and regular nucleic acid tests should be prioritized, and further studies are needed to identify the infectivity of patients. In addition, a potential myocardial microcirculation injury was also observed in Patients A and B, so the long-term sequelae of cardiovascular damage and psychological problems should also be carefully considered in such cases.

Funding: Non-Profit Central Research Institute Fund of Chinese Academy of Medical Sciences (No.2020-PT330-005) and Chengdu Municipal Science and Technology Bureau Key R&D Support Program Technology Innovation R&D Project (No.2020-YF05-00133-SN).

doi: 10.46234/ccdcw2021.172

[#] Corresponding author: Zhu Liu, 137949813@qq.com.

[1] Chengdu Workstation for Emerging Infectious Disease Control and Prevention, Chinese Academy of Medical Sciences, Chengdu, Sichuan, China; [2] Public Health Clinical Center of Chengdu, Chengdu, Sichuan, China; [3] Chengdu Center for Disease Control and Prevention, Chengdu, Sichuan, China.
[&] Joint first authors.

Submitted: May 07, 2021; Accepted: June 09, 2021

REFERENCES

1. National Health Commission. Diagnosis and treatment protocol for COVID-19 (Trial Version 5). http://www.nhc.gov.cn/xcs/zhengcwj/202002/3b09b894ac9b4204a79db5b8912d4440.shtml. [2020-2-5]. (In Chinese).
2. Moncunill G, Mayor A, Santano R, Jiménez A, Vidal M, Tortajada M, et al. SARS-CoV-2 seroprevalence and antibody kinetics among health care workers in a Spanish hospital after 3 months of follow-up. J Infect Dis 2021;223(1):62 – 71. http://dx.doi.org/10.1093/infdis/jiaa696.
3. He ZY, Ren LL, Yang JT, Guo L, Feng LZ, Ma C, et al. Seroprevalence and humoral immune durability of anti-SARS-CoV-2 antibodies in Wuhan, China: a longitudinal, population-level, cross-sectional study. Lancet 2021;397(10279):1075 – 84. http://dx.doi.org/10.1016/S0140-6736(21)00238-5.
4. Zhou W, Xu XM, Chang ZG, Wang H, Zhong XF, Tong XL, et al. The dynamic changes of serum IgM and IgG against SARS-CoV-2 in patients with COVID-19. J Med Virol 2021;93(2):924 – 33. http://dx.doi.org/10.1002/jmv.26353.

Notifiable Infectious Diseases Reports

Reported Cases and Deaths of National Notifiable Infectious Diseases — China, September, 2021

Diseases	Cases	Deaths
Plague	0	0
Cholera	0	0
SARS-CoV	0	0
Acquired immune deficiency syndrome*	5,039	1,963
Hepatitis	125,821	58
Hepatitis A	1,105	1
Hepatitis B	101,701	49
Hepatitis C	20,125	6
Hepatitis D	26	0
Hepatitis E	2,033	2
Other hepatitis	831	0
Poliomyelitis	0	0
Human infection with H5N1 virus	0	0
Measles	85	0
Epidemic hemorrhagic fever	291	0
Rabies†	13	14
Japanese encephalitis	63	1
Dengue	4	0
Anthrax	58	0
Dysentery	5,159	0
Tuberculosis	67,812	124
Typhoid fever and paratyphoid fever	786	0
Meningococcal meningitis	2	0
Pertussis	1,094	0
Diphtheria	0	0
Neonatal tetanus	1	0
Scarlet fever	1,202	0
Brucellosis	5,932	1
Gonorrhea	11,744	0
Syphilis	45,792	9
Leptospirosis	116	2
Schistosomiasis	5	0
Malaria	49	0
Human infection with H7N9 virus	0	0
COVID-19§	1,264	0
Influenza	35,535	0
Mumps	12,606	0

Continued

Diseases	Cases	Deaths
Rubella	90	0
Acute hemorrhagic conjunctivitis	2,321	0
Leprosy	24	0
Typhus	211	0
Kala azar	17	0
Echinococcosis	296	0
Filariasis	0	0
Infectious diarrhea	90,862	0
Hand, foot and mouth disease	86,635	0
Total	**500,929**	**2,172**

* The number of deaths of acquired immune deficiency syndrome is the number of all-cause deaths reported in the month by cumulative reported AIDS patients.

† Among the 14 deaths of rabies cases, 3 were reported before, 11 were reported in September.

§ The data were from the website of the National Health Commission of the People's Republic of China.

Infectious diarrhea excludes cholera, dysentery, typhoid fever and paratyphoid fever.

The number of cases and cause-specific deaths refer to data recorded in National Notifiable Disease Reporting System in China, which includes both clinically-diagnosed cases and laboratory-confirmed cases. Only reported cases of the 31 provincial-level administrative divisions in the mainland of China are included in the table, whereas data of Hong Kong Special Administrative Region, Macau Special Administrative Region, and Taiwan are not included. Monthly statistics are calculated without annual verification, which were usually conducted in February of the next year for de-duplication and verification of reported cases in annual statistics. Therefore, 12-month cases could not be added together directly to calculate the cumulative cases because the individual information might be verified via National Notifiable Disease Reporting System according to information verification or field investigations by local CDCs.

doi: 10.46234/ccdcw2021.240

Indexed by PubMed Central (PMC) and Emerging Sources Citation Index (ESCI).

The inauguration of *China CDC Weekly* is in part supported by Project for Enhancing International Impact of China STM Journals Category D (PIIJ2-D-04-(2018)) of China Association for Science and Technology (CAST).

CCDC weekly

Vol. 3 No. 46 Nov. 12, 2021

Responsible Authority
National Health Commission of the People's Republic of China

Sponsor
Chinese Center for Disease Control and Prevention

Editing and Publishing
China CDC Weekly Editorial Office
No.155 Changbai Road, Changping District, Beijing, China
Tel: 86-10-63150501, 63150701
Email: weekly@chinacdc.cn

CSSN
ISSN 2096-7071
CN 10-1629/R1